Machining Error Analysis with the Consideration of Static Machine Stiffness

LIHANG YANG

Thesis submitted to the University of Nottingham for the degree of Master of Research
Written under the supervision of Dr. HAONAN LI

SEPTEMBER 2022

Abstract

In previous studies on machine tool errors, most efforts mainly focused on modelling of geometric and thermal errors of the machine tool. The machining-force-induced error, however, is gradually becoming unneglectable in modern manufacturing because the increasing kinds of difficult-to-cut materials are used especially in the fields such as aerospace, energy, and automotive, and significant machining forces are generated during machining processes of these materials. Most previous efforts on this topic were based on finite element method, which cannot provide the explicit understanding of the relationship between machine tool error and machine stiffness. To fill this gap, this thesis proposes a physical model of force-induced machine tool errors by utilizing homogeneous error matrix and statics analysis. Theoretical results calculated by the proposed model are compare with the ones calculated by finite element method to prove the model feasibility and accuracy.

Keywords: Machining Error, Physical Modeling, Static Stiffness, Deformation, **Homogeneous Matrix, Differential transformation**

Acknowledgements

I would like to thank my primary advisor during my study in MRes program, Dr. Haonan Li, and other members in my advising group, Dr. Gongyu Liu, and Dr. Chung Ket Thein for their great help in composing and writing this thesis.

Contents

List of Figures

List of Tables

Chapter 1 Introduction & Methodology

1.1 Introduction and background

Machine tools are the foundation of most industries because machine tool accuracy determines machined parts' dimensional accuracy, geometrical consistency, and surface quality. This might also explain why the machine tool market is continuously increasing, although this industry has been developed for already more than 200 years.

According to Grand View [1], the global machine tools market size was valued 77.22 billion USD in 2021 (among which 10.3 billion (Fig.1) in the U.S.) and is expected to grow with the compound annual growth rate of 5.7%. The primary reason driving this increase might attribute to the urgent need from either aerospace, automobile, or even defense sectors, where high-precision metal parts are highly needed.

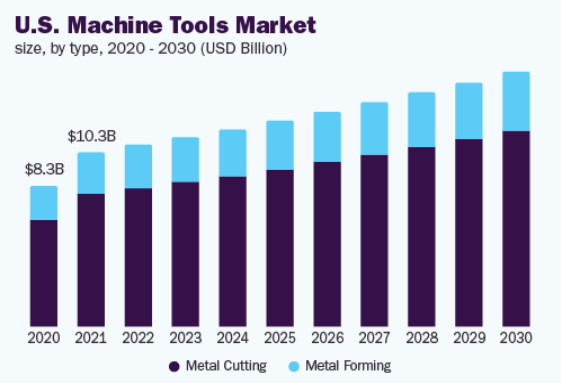

Figure 1 US Market size [1].

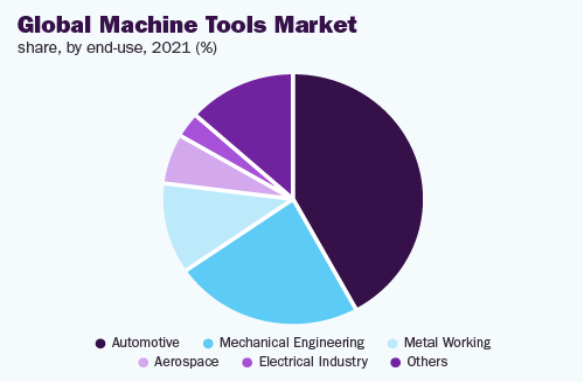

Figure 2 Global machine tools segmentation [2].

Although diverse elements might influence the overall quality of machined workpiece, the machine tool errors might still be considered as the most dominant element [2]. It includes machine tool assembly error, mechanical performance error, thermal error, force-induced machining error. Among all those errors, the key one is force-induced machining error also commonly refer as machining error. Force-induced machining errors can significantly impact the accuracy and quality of machined parts. These errors arise due to various forces acting on the machine tool, cutting tool, and workpiece during the machining process. The force-induced machining errors affect machining accuracy by causing deflection in cutting tools, machine tool, workpiece, and leads to chatter or vibration, thermal effect, tool wear.

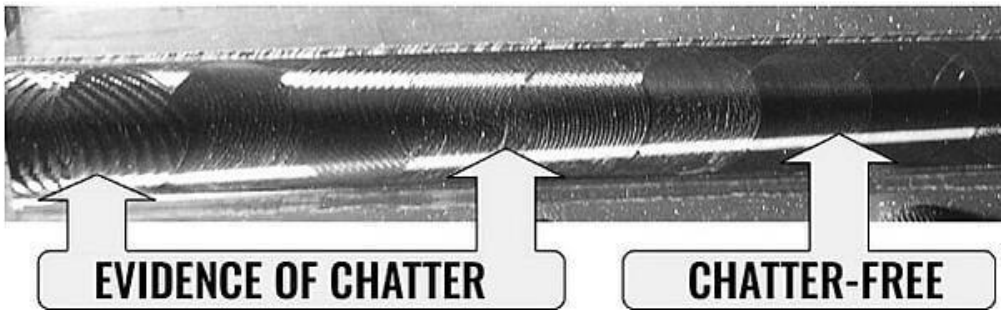

Figure 3 Milling chatter of milling process induced by machining error [36].

One of the most common outcomes demonstrating the existence of force-induced machining error is the chatter mark on workpiece after milling (Fig.3). Chatter is a machining force induced vibration that occurs when the cutting tool engages with the workpiece, causing an uneven cutting action. This can result in a series of unwanted marks on the surface of the workpiece, known as chatter marks. Chatter marks can affect the surface finish, dimensional accuracy, and overall quality of the workpiece. The marks can be visible to the naked eye and can be a sign of poor machining quality. To avoid chatter marks, it is important to find the appropriate machining parameters through studying and minimizing machining force induced error.

Regrettably, force induced machining error has been neither deeply nor widely investigated in the past time, however with the rapid improvement of modern manufacturing standard, the deep understanding of such error should be clearly identified due to the increasing demand for versatile high precision products from aerospace industry (Fig.2) to car manufacturing.

The main motivation for this thesis is to find how machining force affects the precision of machining process by constructing a physical (analytical) model involving classic machining error transformation matrix and machine tool static stiffness. Also, by using physical modeling to study the relationship between force-induced machining error and design of machine tool parts.

1.2 Methodology

This study is focused on force-induced machining error analysis by constructing a physical (analytical) model utilizing static stiffness of the machine tool. Physical modeling on machining error analysis will be a correlation of force-induced machining error and static stiffness of experimented machine tool.

Tool-workpiece displacement error is a representation of force-induced machining error, mathematical homogenous error transformation matrix will be used to describe the functional relationship between tool-workpiece displacement and machine tool deformation.

Static stiffness is not a material property, it is a property of a mechanical system, such as a machine tool, that relates the amount of force applied to the system to the resulting displacement or deflection of the system. It is a measure of the system's ability to resist

deformation or deflection under an applied load. For simple structures like beams or plates, load-deflection method can be used to find the stiffness. For this study, static stiffness of machine tool parts will be calculated using length-deflection method in a simulation software. The functional relationship between machine tool deformation and static stiffness will be obtained.

To construct the final physical (analytical) model of force-induced machining error, correlate the above two functional relationships, to eventually get the functional relationship between force-induced machining error (tool-workpiece displacement) and static stiffness of machine tool.

Validation of physical modeling will be given by using simulation software to further calculate the tool-workpiece displacement error and compare with calculated result from physical (analytical) model. The best way to further validate physical modeling is to take direct measurement from the real machine tool, but due to the limitation of the testing equipment and funding, this study has to use simulation software for validation within the fixed time of this program. Therefore, direction measurement validation will be left for future work.

Chapter 2 Literature Review

2.1 Literature review on Geometric (volumetric) error and many-body system of a machine tool

For machine error representation, Zhu et al. [3] presented an error modeling method by regarding a machine tool as a rigid multi-body system. Commonly 21 geometric errors for a 3-axis machine tool were identified and measured based on a laser interferometer. As shown in Fig.4, each moving part includes positioning and straightness errors on the translational axis, and roll, pitch, yaw error on the rotational axis, plus additional perpendicularity errors between every two axes. Therefore, a typical 3 axis machine tool will have seven errors for each axis multiplies three axes, with a total of 21 geometrical errors.

For more complex multi-axis machine tools such as 5 axis machine tools with rotary table, each additional rotation axis has 6 geometric errors and commonly those errors can be measured by ball-bar [4]. According to rotary table's error direction, it can be classified as radial motion error, axial motion error, tilt motion error and angle positioning error in Fig.5. Fig.5 (a) shows the error motions of axis of rotation, and Fig.5 (b) shows the position and orientation errors (axis shift) of axis average line. Using a 4-by-4 homogeneous transformation matrix to represent the transformation relation between a pair of adjacent bodies is widely adopted, as shown in Fig.6, in such representation each circle which represents an individual physical body transformation in machine tool can be described by a transformation matrix. Some other identification methods have also been used, such as twelve-line method [5] based on a laser interferometer. Measuring and identification of geometric errors is essential for error compensation, and in this field much research have been done using homogenous transformation matrix to define the error transformation between frames [5,7,8-10]. The way to connect each frame in the kinematic chain has been introduced in most related studies is multibody system [3,11] composed of many rigid bodies which can be treated as a universal method on solving machine tool error problems.

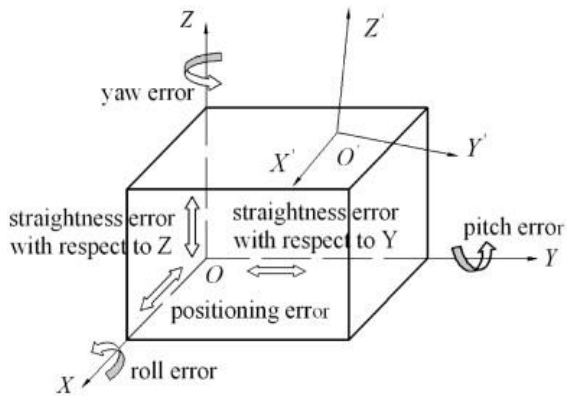

Figure 4 Geometric error for three translational axes [3].

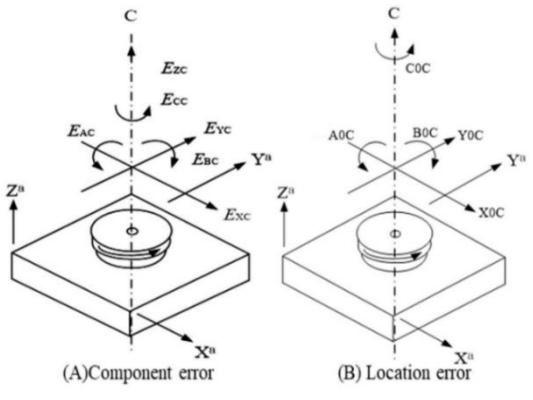

Figure 5 Geometric error for rotary table [32][33].

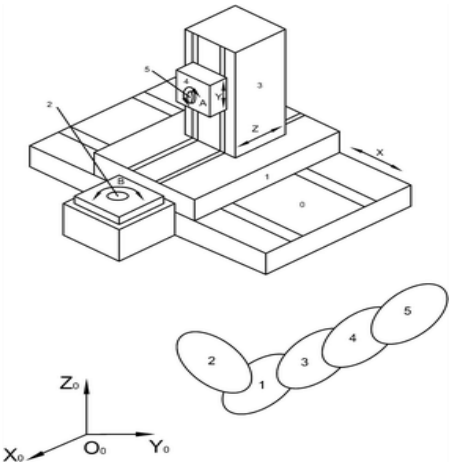

Figure 6 Many-body system of a five-axis machine tool [34].

To show how homogenous transformation matrix works, define X-axis motion translational error $\delta_x(X)$, $\delta_y(X)$, $\delta_z(X)$, and corresponding rotational error, $\varepsilon_x(x)$, $\varepsilon_y(x)$, $\varepsilon_z(x)$, offset parameter $O_x(x)$ corresponds to displacement in X direction. The physical meaning of translational error term is to represent the displacement in the X, Y, and Z direction between the tool coordinate system and the machine coordinate system, when these elements appear firstly, they indicate the translation of the tool coordinate system in relation to the machine coordinate system. Likewise, rotational error elements physically represent the rotational errors or misalignments around the X, Y, and Z axis between the tool coordinate system and the machine coordinate system. The offset parameter physically presents the scaling errors or changes in size along the X, Y, and Z direction between the tool coordinate system and the machine coordinate system (Fig.7). So, the generalized HTM for real motion along the X-axis is given in matrix T:

$$T = \begin{bmatrix} 1 & -\varepsilon_z(x) & \varepsilon_y(x) & X+\delta_{x1}(x) \\ \varepsilon_z(x) & 1 & -\varepsilon_x(x) & \delta_{y1}(x) \\ -\varepsilon_y(x) & \varepsilon_x(x) & 1 & \delta_{z1}(x) \\ 0 & 0 & 0 & 1 \end{bmatrix} \quad (1)$$

When moving from one coordinate system to another, there also exists perpendicular errors; for instance, when a coordinate system in X axis moves from previous Y axis or Z axis there is one perpendicular error either γ_{xy} or γ_{xz}, to take this perpendicular error into consideration and represent in a new matrix T_x:

$$T_x = \begin{bmatrix} 1 & -\gamma_{xy} & \gamma_{xz} & O_x(x) \\ \gamma_{xy} & 1 & 0 & O_y(x) \\ -\gamma_{xz} & 0 & 1 & O_z(x) \\ 0 & 0 & 0 & 1 \end{bmatrix} \cdot \begin{bmatrix} 1 & -\varepsilon_z(x) & \varepsilon_y(x) & X+\delta_{x1}(x) \\ \varepsilon_z(x) & 1 & -\varepsilon_x(x) & \delta_{y1}(x) \\ -\varepsilon_y(x) & \varepsilon_x(x) & 1 & \delta_{z1}(x) \\ 0 & 0 & 0 & 1 \end{bmatrix} \quad (2)$$

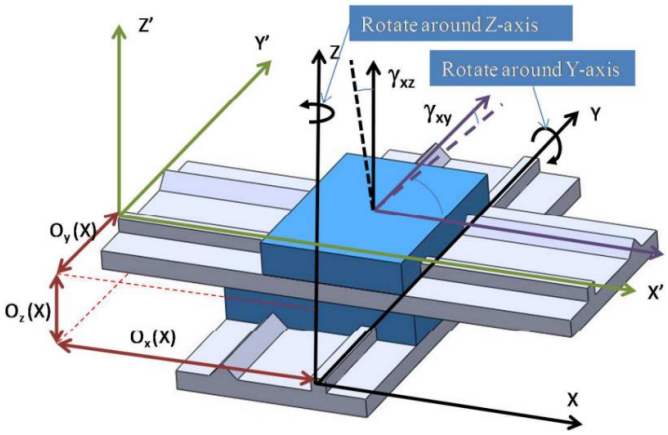

Figure 7 Orientation error of the X axis [35].

For machine tool geometric error model validation, direct measurement of the machine tool error is generally performed by using a measuring device, as mentioned earlier in this chapter [3,4], to record the actual tool path error value during the machining process, then comparing with predicted values obtained through modeling.

Applying direct measurement to validate a geometric error model, the machine tool is first calibrated to establish a baseline reference position. Then, measurements are taken using specialized equipment, such as laser interferometers or ball bars shown in Fig.8, to quantify the magnitude and direction of various error components, such as straightness, flatness, or squareness. Direct measurement plays an important role in geometric machine tool error analysis by providing a quantitative and objective means of assessing machine tool performance.

Figure 8 Calibration from Renishaw QC20 ball-bar

2.2 Literature review on matrix summation in error analysis

Homogeneous transformation matrix as described in pervious literature reviews is wildly used methodology for modeling and error compensation for multi-axes machine tools, but the drawback of this method is also very transparent and pointed out by S. Suh in his research which is heavy symbolic manipulation of the matrix multiplication [12]. Therefore, in another

study on modelling of five-axis machine tool metrology model conducted by Y. Lin and Y. Shen along with other research groups [13,14,15] introduced matrix summation approach to replace the HTM method. This approach breaks down the kinematic equation into six components, each of which has clear physical meaning, reduces computations and is more understandable. In order to perform this summation method, Kiridena and Ferreira classified 5-axis machines into different types of error analysis sequence, known as TTTRR, RTTTR and RRTTT systems then perform Denavit-Hartenberg convention to develop kinematic models for above three machine configurations [16]. Here, we define T as translational error and R as rotational error. For example, TRRRT (Fig. 9(b)) stands for Translation-Rotation-Rotation-Rotation- Translation. The two rotary axes are separated, one connects with the cutting tool, other one connects to the machine bed, the characteristics of TRRRT lies between TTTRR and RRTTT. This error sequence refers to the five geometric errors in the following order: X-axis straightness error, Y-axis straightness error, Z-axis straightness error, pitch error, and roll error. Srivastava et al. [17] also adopted this convention focused on tool error for machine type TTTRR.

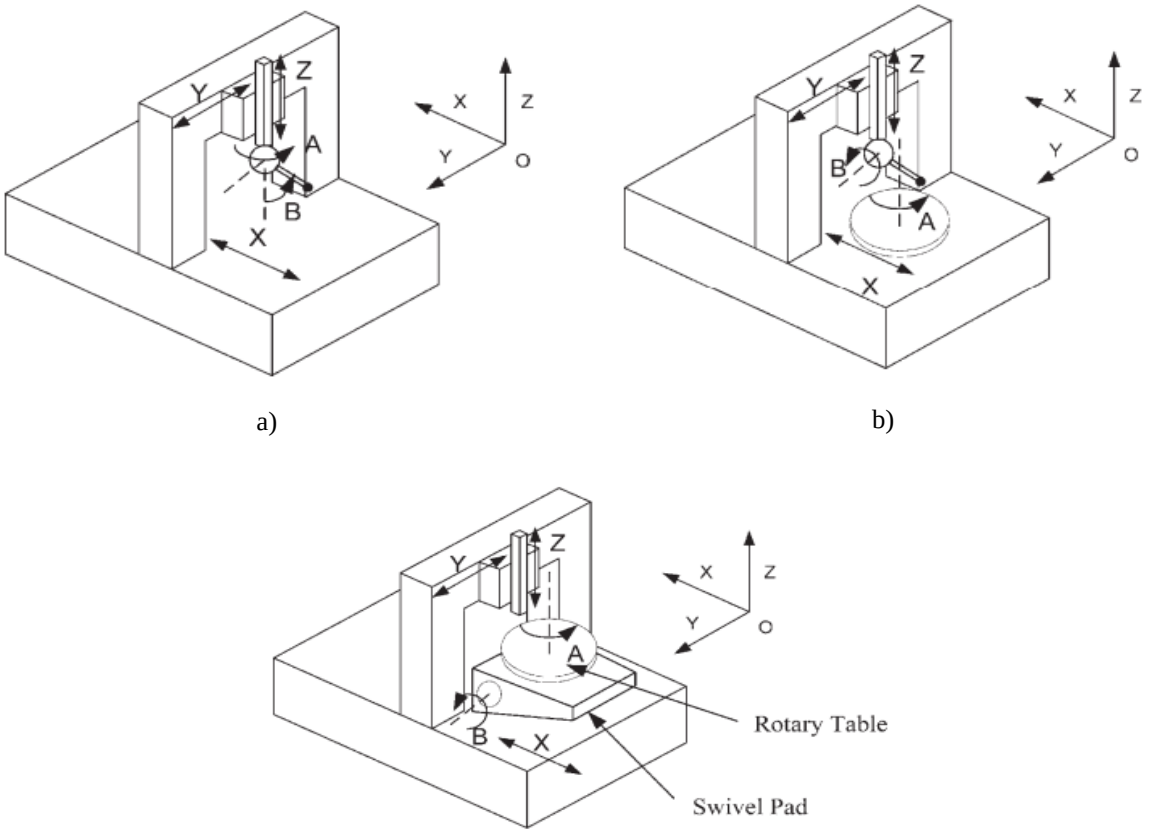

Figure 9 Layout for TTTRR a), RTTTR b), RRTTT c) machine type [16].

Generalizing above three machine tool configurations, TTTRR RTTTR RRTTT, the generic form of the kinematic models for the five-axis systems can be written as:

$$P_{system} = P_{ideal} + P_{a\ error} + P_{b\ error} + P_{x\ error} + P_{y\ error} + P_{z\ error} \quad (3)$$

By Reviewing the kinematic model in the fig. 5 below, the contribution of the error motions of the translation axes to the volumetric errors of the machine is clear, and contributions from different part (error term) of the machine can be regarded as the corresponding three-axis error model transformed by the ideal angular motions of the rotary axes. Simply by switching the location of $P_{a\ error}$ or $P_{b\ error}$, the formulation can represent whether the rotary axis appears before or after the translational axes.

Machines	$Pxyz$
TTTRR (FXYZAB)	$Pxyz = Pxerror + Pyerror + Pzerror = E_{3axis} \cdot Haoffset \cdot Haideal \cdot Hboffset \cdot Hbideal \cdot T$
RTTTR (AFXYZB)	$Pxyz = Pxerror + Pyerror + Pzerror = Haideal^{-1} \cdot E_{3axis} \cdot Hboffset \cdot Hbideal \cdot T$
RRTTT (ABFXYZ)	$Pxyz = Pxerror + Pyerror + Pzerror = Haideal^{-1} \cdot Hbideal^{-1} \cdot E_{3axis} \cdot T$

$$E_{FXYZ} = Hxerror \cdot Hyideal \cdot Hzideal + Hyerror \cdot Hzideal + Hzerror$$

$$E_{FXYZ} \cdot T = \begin{bmatrix} xTx + yTx + zTx - (xRz+Sxy) \cdot (Y+Yp) + (xRy+Sxz) \cdot (Z+Zp) + yRy \cdot (Z+Zp) - yRz \cdot Yp + zRy \cdot Zp - zRz \cdot Yp \\ xTy + yTy + zTy - xRx \cdot (Z+Zp) + (xRz+Sxy) \cdot Xp - (yRx+Syz) \cdot (Z+Zp) + yRz \cdot Xp - zRx \cdot Zp + zRz \cdot X \\ xTz + yTz + zTz + xRx \cdot (Y+Yp) - (xRy+Sxz) \cdot Xp + (yRx+Syz) \cdot Yp - yRy \cdot Xp + zRx \cdot Yp - zRy \cdot Xp \\ 1 \end{bmatrix}$$

Figure 10 Contribution of the error motions of translational axes [16].

2.3 Literature review on time dependent error matrix

In error analysis of machine tool, when constructing of homogenous transformation matrix, one assumption has been made through most of the studies which is errors of a joint (axis) are assumed as constant with movement alone the joint. The assumption is not justifiable since substantial variation can be observed, and this situation can be further elevated to geometric error of a machine is time variant [18]. Fig.11 shows the time variant coordinate shifting under geometric error been applied. The machining error An article from Dufour and Groppetti [19] stored each error components from different locations in the machine's workspace by various loading and thermal conditions, then interpolation is used to corelates each stored value. Sata [20] states that a quadratic correlation between the error and coordinates of it. Trigonometric relationship has also been used to describe the correlation of arrival of geometric errors [21]. HTM and rigid body kinematic should be used while considering the transformation of inaccurate links and joints and its time variance [22,23,24,25].

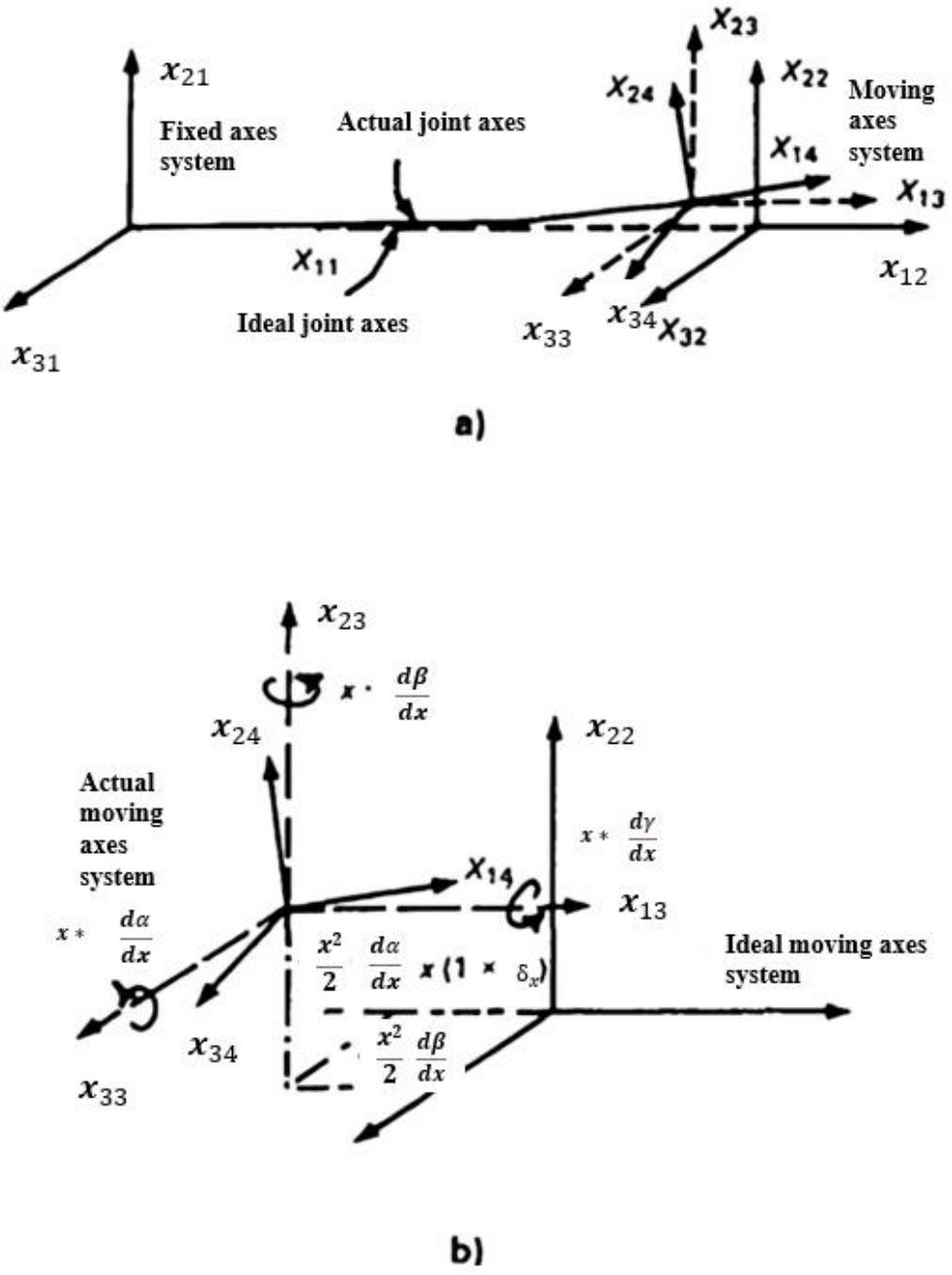

Figure 11 Coordinate Systems on a Prismatic Joint [18].

a) Accurate and Inaccurate joint

b) Magnification of the Moving axes systems

The joint transformation matrix for an inaccurate link can be given:

$$\Phi = \begin{bmatrix} 1 & -\alpha(x) & \beta(x) & x + \Delta x \\ \alpha(x) & 1 & -\gamma(x) & \int_0^x \alpha(x)dx \\ -\beta(x) & \gamma(x) & 1 & \int_0^x -\beta(x)dx \\ 0 & 0 & 0 & 1 \end{bmatrix} \quad (4)$$

Carry out the calculation in the homogeneous transformation matrix can get the residual error matrix as:

$$S = \begin{bmatrix} 0 & -\frac{d\alpha 2}{dx2} & \frac{d\beta 3}{dx3} \\ \frac{d\alpha 1}{dx1} & 0 & -\frac{d\gamma 3}{dx3} \\ -\frac{d\beta 1}{dx1} & \frac{d\gamma 2}{dx2} & 0 \end{bmatrix} \quad (5)$$

When such summation method has been used to rearrange error matrix for links and joints, the expression is developed in quadratic relation based on observations, and the assumption of linear relation between individual error was made. This method can be extended to consider parabolic or cubic variation of the individual errors by modifying the shape and joint for any links.

2.4 Literature review on machine tool stiffness

For machining error simulation in this study, the focus point is constructing physical error model by investigating how the machining force affect the machine stiffness. Then correlate machining error with machine parts deformation utilizing static stiffness. Stiffness is a physical quantity which represent how material respond to various types of loading conditions. It is crucial when comes to machine tool design, improving machining accuracy and reliability [26], therefore securing the maximum static and dynamic stiffness of machine tool will be investigated. Static stiffness analysis can be done through numerical simulation [27] to find the effect of frame deformation on tool tip displacement. Dynamic stiffness of large machine is usually improved by reducing the weight of some parts [28], this method was done by Suh et al. in their research paper. Suh's group used vertical and horizontal slides of a large CNC machine made out of high modulus carbon fiber composite structures, it reduces the weight from 34% to 26% and increased damping by 1.5 to 5.7 times. Numerical analysis of static stiffness has commonly been done through simulation software such as Inventor, CREO, SolidWorks as proposed in many relative research papers [29,30,31]. In Vrtiel's research, the relation between feed rate and machine tool stiffness has been studied using numerical modeling.

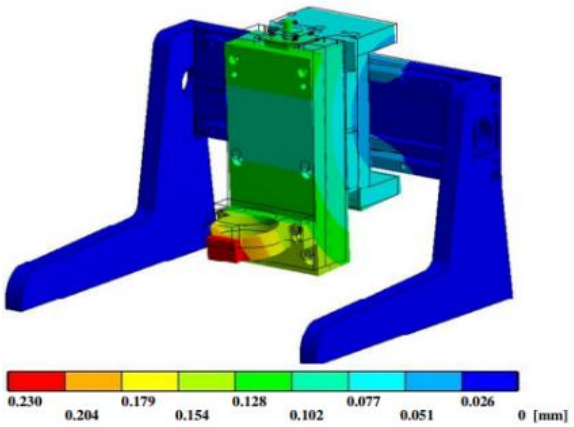

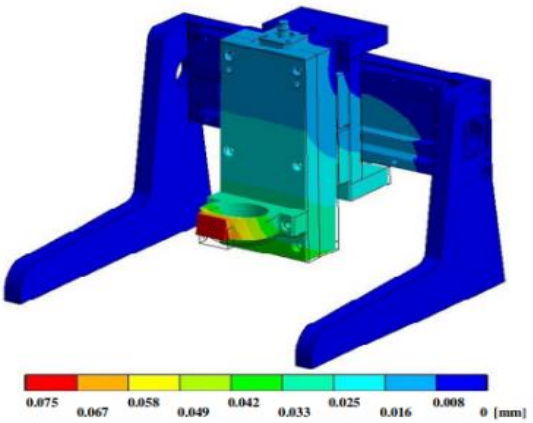

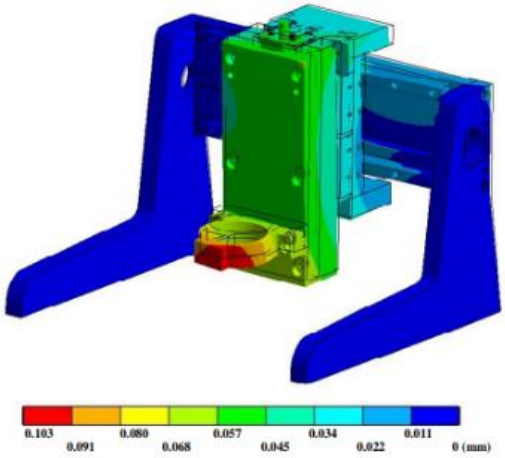

Figure 12 Deformation of the designed frame caused by machining with different feed rate [27].

2.5 Literature review conclusion

For machine error analysis, research has been done by previous groups that are majorly focused on geometrical error and thermal error. When analyzing machine tool geometric error, homogeneous transformation matrix has been used frequently, and such method can be adopted to address tool-workpiece displacement error under machining force. The method which has been deployed to simplify the transformation error matrix is matrix summation. Mathematical models for geometric error analysis are sophisticated, but there is rarely a topic related to force-induced machining error analysis. For stiffness of machine tool, the way to optimize the machine tool design is commonly solving the numerical model in simulation software using numerical analysis, very few study has been done on physical (analytical) modeling of the machine tool. Even though numerical modeling offers a powerful tool for analyzing machine tool errors and optimizing machine tool performance, but still direct measuring remains an important tool for verifying and validating numerical models. In this case, a physical model can be advantageous over a numerical model in analyzing machine tool errors because it allows for direct measurement of the actual machine tool and its components. This can provide a more accurate and precise understanding of the machine tool's behavior, as well as identify sources of error that may be difficult to simulate in a numerical model. Additionally, physical models can provide insights into the dynamic behavior of the machine tool, such as vibration, thermal expansion, and other factors that may be difficult to capture in a numerical model.

Chapter 3 Machining error model for high-speed 3-axis milling machine

3.1 Basic principle of force-induced machining error physical modeling

As the reviewed articles show that force-induced machining error during the machining process is commonly not discussed, one of the reasons will be the force is comparatively small and resultant deflection could be neglected in finished machining. But modern industrial parts in specific areas like aerospace and aviation require to use hardened steel or materials that referred as difficult-to-cut, difficult-to-machine such as high temperature Ni-based alloy or Co-based alloy. In such case, during the machining operation, the machining force could be large, and the force generated during the action is impossible to ignore.

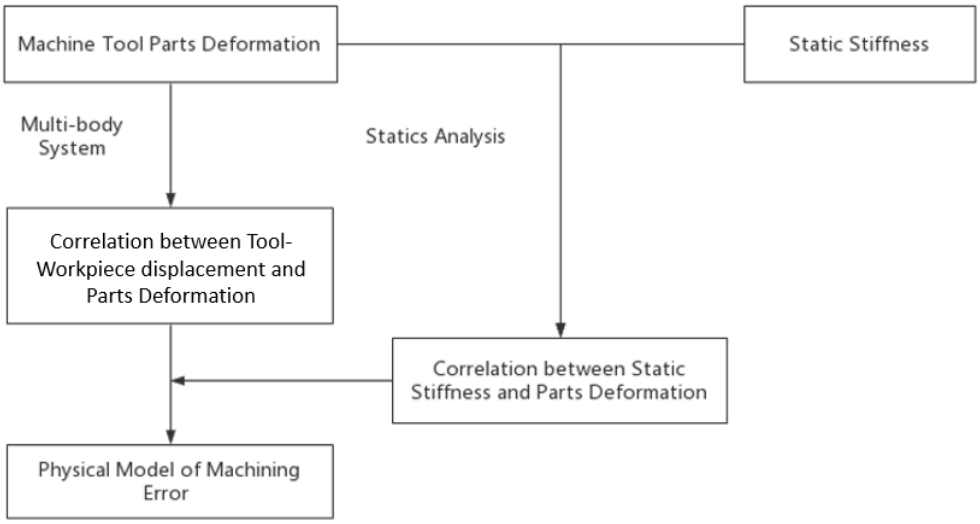

Figure 13 Flow Chart for physical error modeling.

The stiffness of all the components of the machine tool is responsible for error caused because of the machining action, especially when the force is considerably large. Due to the different stiffness that each part of the machine tool has, the selection of material and structural design of the machine tool needs to be considered. As a result of the machining force, the relative displace between workpiece and tool varies on account of the distortion of the different elements of the machine. Different stiffness of the parts from the machine will contribute differently to the accuracy of the machining process. For given stiffness of the whole structure, larger machining force will cause lower machining accuracy, increasing machining error.

The static stiffness of the machine tool parts is usually calculated by length-deflection method, or some of the manufacturers may provide in their manufactural handbook. Thus, for a given stiffness, the correlation between the machining force and deformation of the machine tool parts (namely bed, column, spindle, guideway etc.) can be described by using statics equilibrium equations.

Homogeneous transformation matrixes (HTM) are commonly used while analyzing the geometric error of machine tool, here same logic applies, HTMs will be utilized to address the functional correlation between relative tool-workpiece displacement and part deformation. Ultimately, through correlating the above two equations, the functional relationship between relative tool-workpiece displacement (machining error) and structural stiffness can be obtained.

3.2 Generalized homogeneous transformation matrix for machine tool

For a machine assembly, we consider six error parameters for a translational moving axis, namely three linear errors and three rotational errors. Taking X-axis as an example, errors associated with this single axis while moving can be expressed as [δ_{xx}, δ_{yx}, δ_{zx}, ε_{xx}, ε_{yx}, ε_{zx}]. Since the geometric errors are small, so based on differential transformation theory, they can be equivalent to differential movement from its ideal position, and the differential movement commonly can be referred as Δ_x in error analysis:

$$ {}^{0}T'_{1} = {}^{0}T_{1} + d({}^{0}T_{1}) = {}^{0}T_{1} + {}^{0}T_{1}\,{}^{0}\Delta_{1} \quad (6) $$

Here, ${}^{0}T'_{1}$ stands for the actual transformation with error parameters from a coordinate system "0" moves to another coordinate system "1". To extend this relation with different error parameters in matrix form:

$$ [{}^{0}T'_{1}] = \begin{bmatrix} 1 & -\varepsilon_{z1}(x) & \varepsilon_{y1}(x) & a_1 + \delta_{x1}(x) + \Delta_{x1} \\ \varepsilon_{z1}(x) & 1 & -\varepsilon_{x1}(x) & b_1 + \delta_{y1}(x) \\ -\varepsilon_{y1}(x) & \varepsilon_{x1}(x) & 1 & c_1 + \delta_{z1}(x) \\ 0 & 0 & 0 & 1 \end{bmatrix} \quad (7) $$

In above matrix:

$\varepsilon_{x1}(x)$ represents roll error for assembly in coordinate system 0

$\varepsilon_{y1}(x)$ represents pitch error for assembly in coordinate system 0

$\varepsilon_{z1}(x)$ represents yaw error for assembly in coordinate system 0

$\delta_{x1}(x)$ represents position error in moving direction (X direction) for assembly in coordinate system 0

$\delta_{y1}(x)$ represents horizontal straightness error for assembly in coordinate system 0

$\delta_{z1}(x)$ represents vertical straightness error for assembly in coordinate system 0

a_1 represents the offset parameters in X direction between origins in coordinate system 1 and 0

b_1 represents the offset parameters in Y direction between origins in coordinate system 1 and 0

c_1 represents the offset parameters in Z direction between origins in coordinate system 1 and 0

Δ_{x1} represents the displacement for assembly in coordinate system 0 moving towards X direction

3.3 Force-induced machining (Tool-Workpiece displacement) error modelling for a 3-axis high-speed milling machine

In this study, a 3-axis milling machine will be used to illustrate the proposed machining error modeling method. Since 3-axis machines are generally less expensive than 5-axis machines, making them a more affordable option for many manufacturers. Most machining operations only require 3-axis machining, such as milling flat surfaces, drilling holes, or creating simple shapes. For machining error analysis, 3-axis machine tool is simpler in design and operation, also has fewer sources of error. By adopting the identical methodology, the physical model of 3-axis machine tool can be quickly extended to 5-axis machine tool.

A 3-axis high-speed milling machine's 3D CAD model with machine tool dimensions and material specifications are given (Table 1) from a local machine tool company which is currently working with our research group to perform structural analysis and optimization. The company is named JingWei CAD/CAM, and the 3-axis high-speed milling machine used in this study has model name CB03II-2516-RQ show in Fig.14(a). There are a total of three moving axes (X-axis, Y-axis, Z-axis), and the workpiece has been fixed on the transitional belt by an air compressor under the machine bed. During the machining process, the transitional belt is also fixed on the working platform by air compressor, only the crossbeam is moving freely to operate.

a)

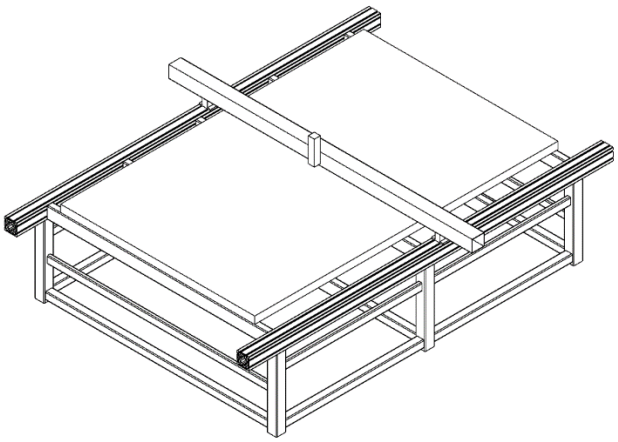

b)

Figure 14 a) actual photo of 3-axis high-speed milling machine from JingWei CB03II-2516-RQ

b) drawn figure of 3-axis high-speed milling machine from JingWei CB03II-2516-RQ

To analyze the kinematic chain of the machine tool, define the first coordinate system, 0-$X_0Y_0Z_0$ labelled "1" in Fig.15, representing the machine bed which has been fixed on the ground and all other components are mounted on it. Coordinate system O_1 which label "2" will be defined as the cross beam (gantry), which are the parts mounted on the work platform move horizontally in X direction. O_2 which labelled "3" will be defined as the head on the cross beam, driven by an electron motor and moves longitudinally in Z direction. O_3 which labelled "4" is the coordinate system on the linkage between the head and spindle, which drives the spindle to move vertically in Y direction. Workpiece has been fixed by air compressor on the transitional belt has its coordinate system O_w which labelled "5", cutting tools are mounted on the spindle with its coordinate system O_t. Through the kinematic chain of this machine tool, there exists two paths to demonstrate machining error. First, since coordinate system O_0 is the machine tool bed fixed on the ground, all other parts of this machine are assembled on it, there exists a path, begin with O_0 and end with O_w. Another path will be start with O_0, transfer to cross beam O_1, and further transfer to longitudinally moved machine head coordinate O_2, then to spindle O_3, cutting tool is mounted on the spindle, has its coordinate O_t. If there doesn't exist machining error, the end of these two kinematic chains will remain on the same position in space. For a given coordinate in O_1, to bring it down to O_0 coordinate system with its real position in machining space by multiplying the error matrix Δ_1 has been shown in above example.

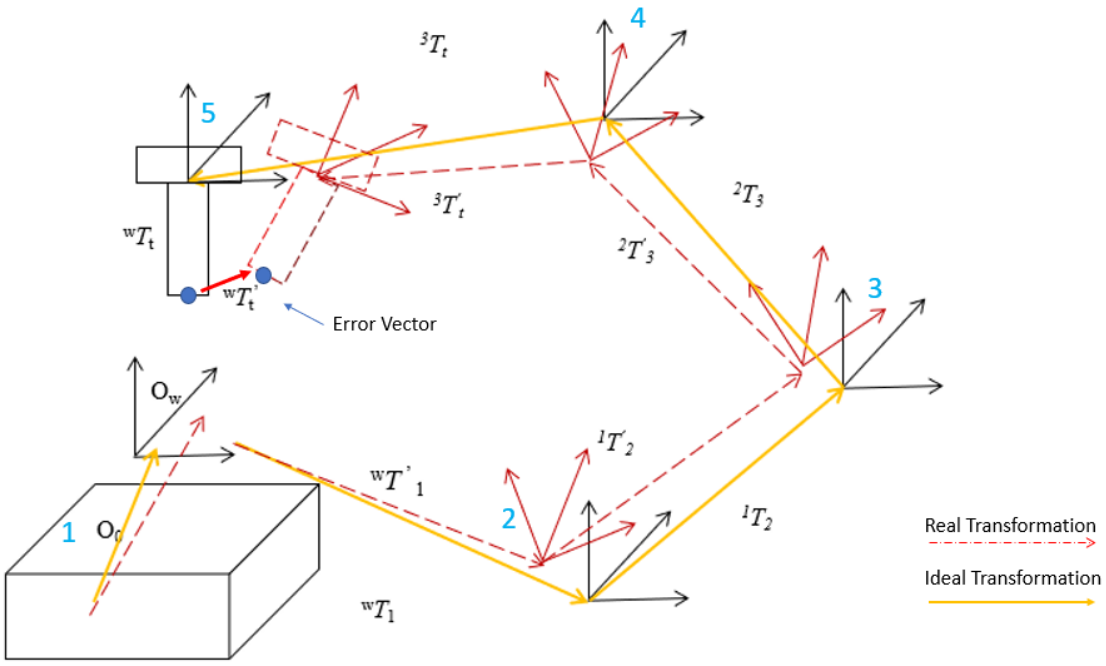

Figure 15 Error propagation from workpiece to tool.

$$[{}^{0}\mathrm{T'}_{1}] = \begin{bmatrix} 1 & -\varepsilon_{z1}(x) & \varepsilon_{y1}(x) & a_1 + \delta_{x1}(x) + \Delta_{x1} \\ \varepsilon_{z1}(x) & 1 & -\varepsilon_{x1}(x) & b_1 + \delta_{y1}(x) \\ -\varepsilon_{y1}(x) & \varepsilon_{x1}(x) & 1 & c_1 + \delta_{z1}(x) \\ 0 & 0 & 0 & 1 \end{bmatrix} \quad (8)$$

Follow the same logic, one can get:

$$[{}^{1}\mathrm{T'}_{2}] = \begin{bmatrix} 1 & -\varepsilon_{z2}(z) & \varepsilon_{y2}(z) & a_2 + \delta_{x2}(z) \\ \varepsilon_{z2}(z) & 1 & -\varepsilon_{x2}(z) & b_2 + \delta_{y2}(z) + \Delta_{y2} \\ -\varepsilon_{y2}(z) & \varepsilon_{x2}(z) & 1 & c_2 + \delta_{z2}(z) \\ 0 & 0 & 0 & 1 \end{bmatrix} \quad (9)$$

$$[{}^{2}\mathrm{T'}_{3}] = \begin{bmatrix} 1 & -\varepsilon_{z3}(y) & \varepsilon_{y3}(y) & a_3 + \delta_{x3}(y) \\ \varepsilon_{z3}(y) & 1 & -\varepsilon_{x3}(y) & b_3 + \delta_{y3}(y) \\ -\varepsilon_{y3}(y) & \varepsilon_{x3}(y) & 1 & c_3 + \delta_{z3}(y) + \Delta_{z3} \\ 0 & 0 & 0 & 1 \end{bmatrix} \quad (10)$$

$$[{}^{0}\mathrm{T'}_{t}] = [{}^{0}\mathrm{T'}_{1}]\,[{}^{1}\mathrm{T'}_{2}]\,[{}^{2}\mathrm{T'}_{3}]\,[{}^{3}\mathrm{T'}_{t}] \quad (11)$$

$$[{}^{0}\mathrm{T'}_{w}] = [{}^{0}\mathrm{T'}_{t}]\,[\mathrm{E_v}] \quad (12)$$

$$[\mathrm{E_v}] = [{}^{0}\mathrm{T'}_{t}]^{-1}\,[{}^{0}\mathrm{T'}_{w}] \quad (13)$$

3.4 Machine tool stiffness modeling

3.4.1 Statics analysis for crossbeam

Stiffness of the whole machine tool assembly has been introduced here because most of the modern studies have shown that error compensation towards geometric error and thermal deformation already significantly improved machining accuracy. But the argument here is due to the high precision requirement in areas like aerospace, will need materials like hardened steel, nickel alloy to be machined with extremely high accuracy such as 5μm in machining error. Under these market needs, to achieve such high precision during the machining process, force induced machining error should be explored. Comparatively much larger machining force will be introduced during the machining process, and such force will cause machine tool assembly to deform and lower the machining accuracy.

For the milling machine in this study, the most vulnerable part will be the cross beam, it is combined with beam frame and upper and down rails which are guide screws (ball screw). The guide screws drag the spindle and cutting tool move horizontally over the workpiece. The weight of spindle and machine head components are acting on the cross beam.

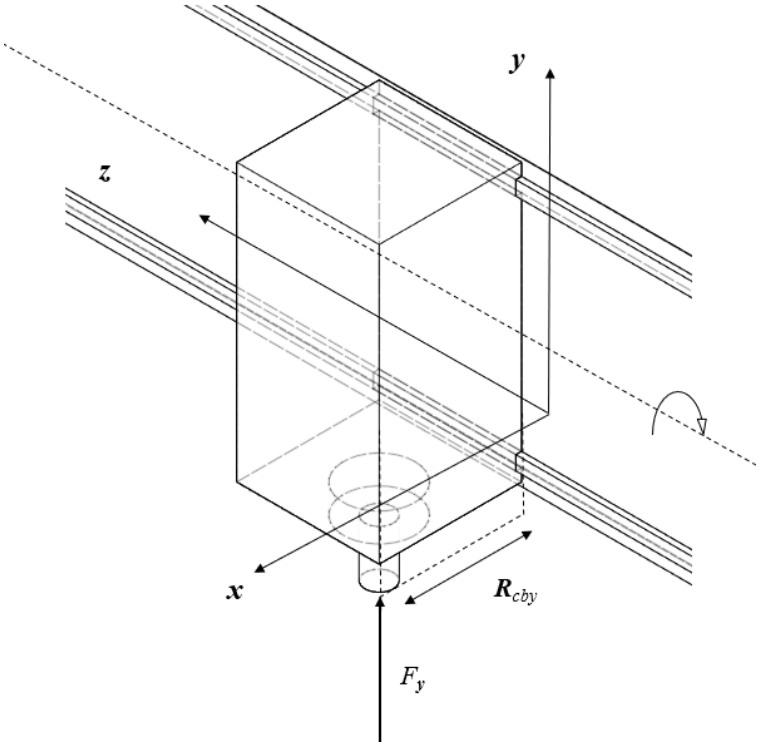

Figure 16 Side view of machine head.

F_y is force in +Y direction

R_{cby} is the force arm of F_y

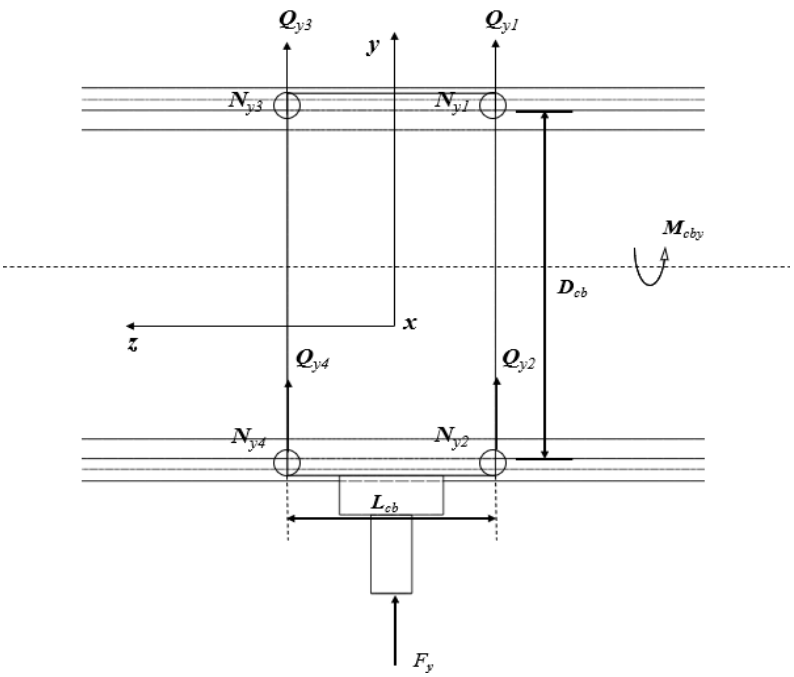

Figure 17 Front view of machine head.

N_{y1} to N_{y4} is the normal force acting on crossbeam

M_{cby} is the moment of F_y

Q_{y1} to Q_{y4} is the shearing on crossbeam

For the cross beam, when the cutting tool experiencing a machining force at direction +Y (Fig.17), it can be treated as a force $+F_y \vec{j}$ and moment of force +Mcby $\vec{k}$, defining the displacement between the force and cross beam (lever arm) Rcby, the moment is the cross product of the displacement and force:

$$M_{cby} \vec{k} = -R_{cby} \vec{j} \times F_x \vec{i} \quad (14)$$

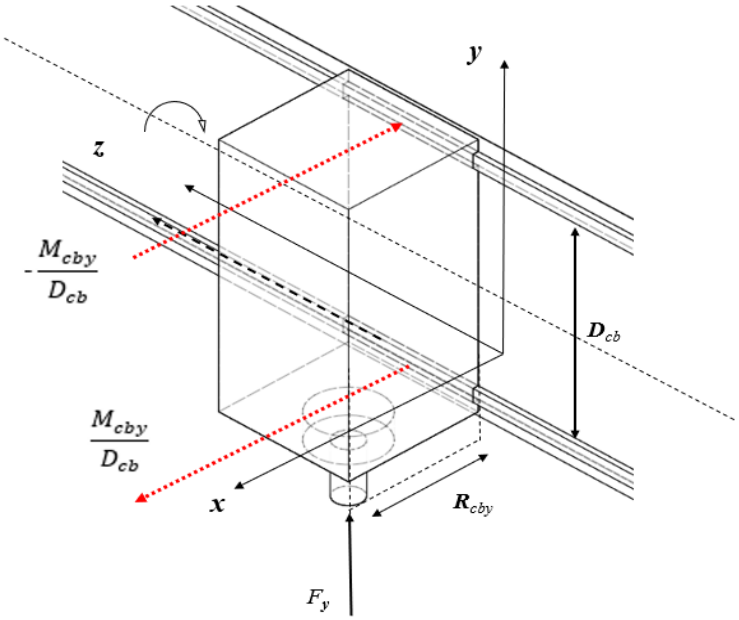

Figure 18 Side view of machine head with +Y directional machining force applied.

$\frac{M_{cby}}{D_{cb}}$ *is the force couple from the moment*

The moment of force is equivalent to a force couple (Fig.18), same magnitude but opposite direction defined as $\pm(\frac{M_{cby}}{D_{cb}})\,\vec{\imath}$, the moment can also be illustrated by replacing the machining force with force couple:

$$M_{cby}\,\vec{k} = D_{cb}\,\vec{j} \times [-(\frac{M_{cby}}{D_{cb}})\,\vec{\imath}] = D_{cb}\,\vec{j} \times 2[-(\frac{F_x R_{cby}}{2D_{cb}})\,\vec{\imath}] \quad (15)$$

D_{cb} is defined as the distance between the rails on the cross beam, point 1 and 2.

Machining Force is divided into 4 equivalent forces and shown in the figure below. At the point 1 and 3, cross beam is experiencing shear force $+(\frac{F_x}{4})\,\vec{j}$ and nominal force $(\frac{F_x R_{cb}}{2D_{cb}})\,\vec{\imath}$, and at the point 2 and 4, it is experiencing the same magnitude of shear force and nominal force but opposite in direction. Nominal force will be denoted by N and shear force will be denoted by Q.

$$N_{y1}\vec{\imath} = N_{y3}\vec{\imath} = [+(\frac{F_y R_{cby}}{2D_{cb}})\,\vec{\imath}] \quad (16)$$

$$N_{y2}\vec{\imath} = N_{y4}\vec{\imath} = [-(\frac{F_y R_{cby}}{2D_{cb}})\,\vec{\imath}] \quad (17)$$

$$Q_{y1}\,\vec{j} = Q_{y2}\,\vec{j} = Q_{y3}\,\vec{j} = Q_{y4}\,\vec{j} = (\frac{F_y}{4})\,\vec{j} \quad (18)$$

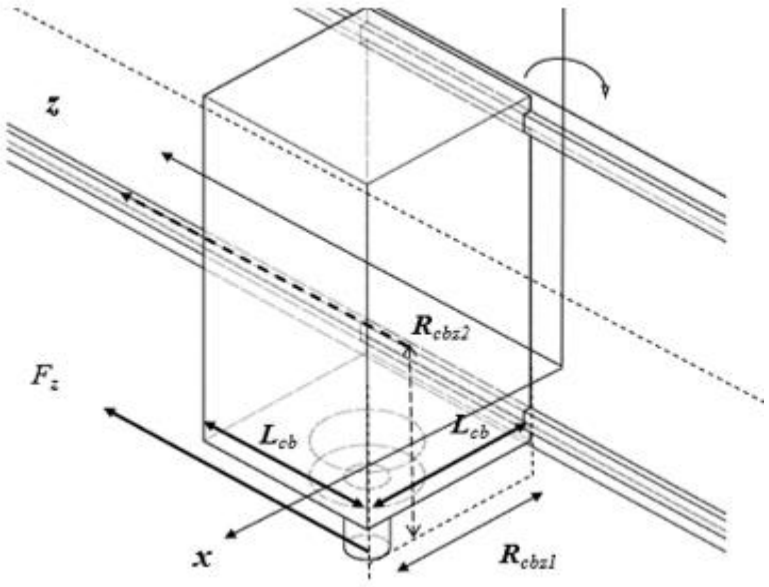

Figure 19 Side view of machine head with +Z directional machining force applied.

Adopting the same logic and analyzing when cross beam experiencing the same machining force but in +Z direction (Fig.19). First, since under the +Z directional force as indicated in the figure above, the machine tool tends to rotate around X axis and Y axis, so the lever arm that generate the torque will be different, and during the calculation, there will be 2 different moments. Introducing a new quantity L_{cb} for defining the new force pair, L is the width of machine head, the distance between point 2 and 4. For the identical points on the beam, one can get the following equation:

Moment of force on X axis:

$$N_{z1}\vec{j} = N_{z2}\vec{j} = [+ (\frac{F_y R_{cbz2}}{2L_{cb}})\,\vec{j}] \quad (19)$$

$$N_{z3}\vec{j} = N_{z4}\vec{j} = [- (\frac{F_y R_{cbz2}}{2L_{cb}})\,\vec{j}] \quad (20)$$

Moment of force on Y axis:

$$Nz1\vec{\imath} = Nz2\vec{\imath} = [- (\frac{F_y R_{cbz1}}{2L_{cb}})\,\vec{\imath}] \quad (21)$$

$$Nz3\vec{\imath} = Nz4\vec{\imath} = [+ (\frac{F_y R_{cbz1}}{2L_{cb}})\,\vec{\imath}] \quad (22)$$

$$Qz1\,\vec{k} = Qz2\,\vec{k} = Qz3\,\vec{k} = Qz4\,\vec{k} = 0 \quad (23)$$

In the case when having Z directional force, the force is acting along the moving direction of the machine head, Z axis, therefore the tangential force, shear force, will not be considered when analyzing the structural deformation of machine tool. The shear force will be causing the deformation of guide screws.

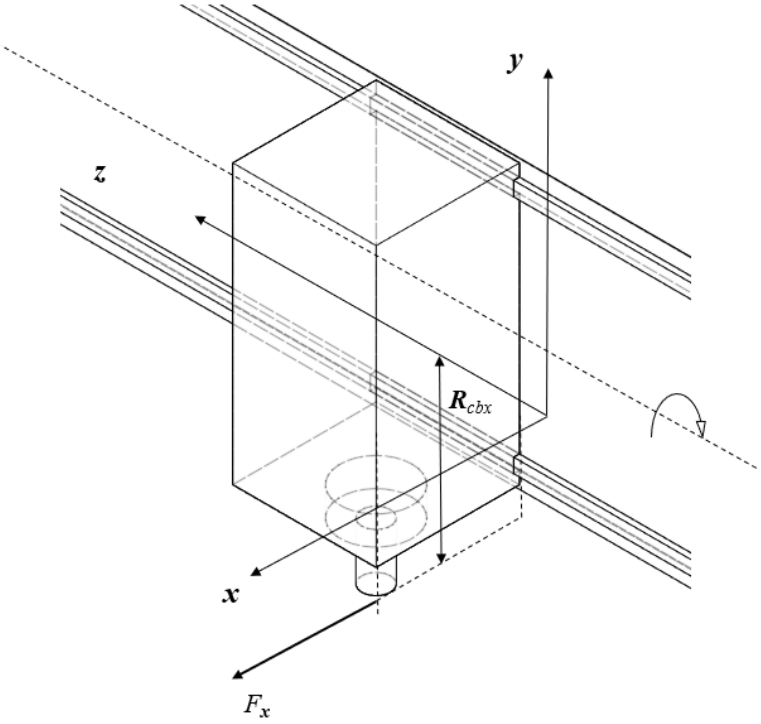

Figure 20 Side view of machine head with +X directional machining force applied.

When cross beam is experiencing +X (Fig.20) unit force, it can be treated as a force $+F_x \vec{\imath}$ and moment of force $-M_{cby} \vec{k}$, defining the displacement between the force and cross beam R_{cbx}, the moment is the cross product of the displacement and force:

$$M_{cbx} \vec{k} = -R_{cbx} \vec{j} \times F_x \vec{\imath} \qquad (24)$$

$$N_{x1}\vec{\imath} = N_{x3}\vec{\imath} = [+ (\frac{F_x R_{cbx}}{2D_{cb}}) \vec{\imath}] \qquad (25)$$

$$N_{x2}\vec{\imath} = N_{x4}\vec{\imath} = [- (\frac{F_x R_{cbx}}{2D_{cb}}) \vec{\imath}] \qquad (26)$$

$$Q_{x1} \vec{j} = Q_{x2} \vec{j} = Q_{x3} \vec{j} = Q_{x4} \vec{j} = + (\frac{F_x}{4}) \vec{j} \qquad (27)$$

3.4.2 Correlation between deformation and machining force for cross beam

With the existing relation between deformation and machining force acting on the cutting tool, since the deformation due to the machining force is small, so based on rigid body transformation, the correlation between force and deformation can be illustrated by Hooke's law. With this relation, one can use equations in section 3.4.1 eventually find the interaction between force-induced error and stiffness of the structure.

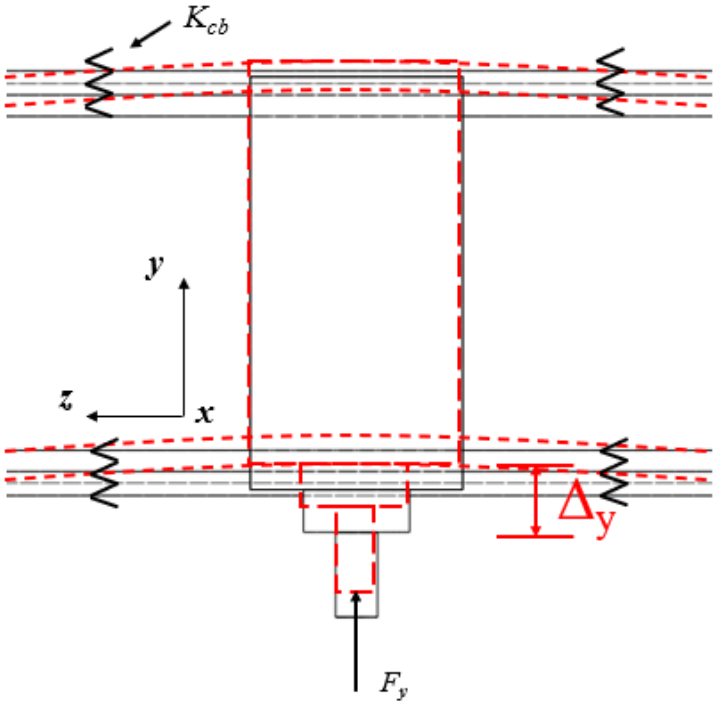

Figure 21 Front view of Machine head deformation due to shear force.

Take cross beam as an example to apply Hooke's Law (Fig.21):

From the equation in 3.4.1, knowing that when a +Y direction unit force applies on the cutting tool, it generates the shear force $Q_{y1}\vec{j} = Q_{y2}\vec{j} = Q_{y3}\vec{j} = Q_{y4}\vec{j} = -(\frac{F_y}{4})\vec{j}$, then it is easy to find the deformation (positional error) for cross beam at Y direction:

$$\Delta y_{cby} = \frac{F_y}{4k_{cby}}\vec{j} \quad (28)$$

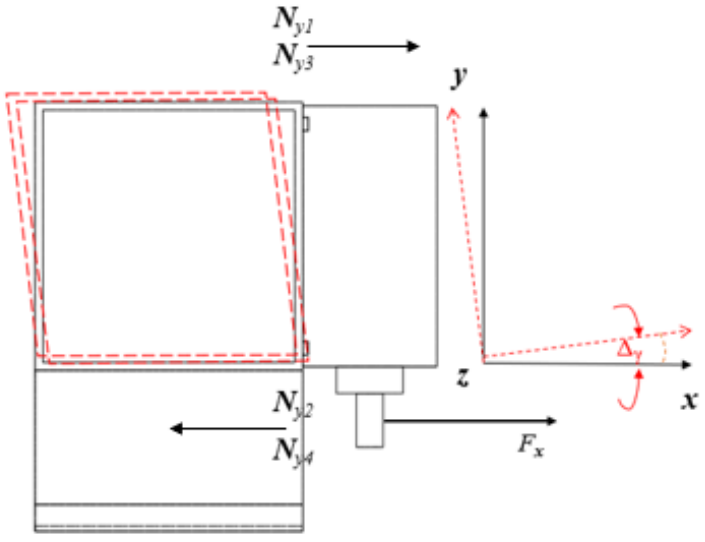

Figure 22 Side view of crossbeam deformation due to torque from +X directional machining force.

Under the same condition, when +Y direction unit force applied (Fig.22), the cross beam tends to rotate around Z-axis and then creates angular error, the pivot point can be treated as the geometrical center of the machine head. From the side view, one can be discovered that two adjoint points, point 1 and 3 will be pulled to the left under the effect of +Y machining force, point 2 and 4 will be pulled to the right. Since the degree of beam rotation is small, so by using small angle approximation, the deformation of the beam due to the moment can be found:

Given $N_{y1}\vec{\imath} = N_{y3}\vec{\imath} = [+ (\frac{F_y R_{cby}}{2D_{cb}})\vec{\imath}]$, the beam rotation caused by +Y directional force will be:

$$\Delta\gamma_{cby} = [(\frac{F_y R_{cby}}{2D_{cb}}) \times \frac{1}{k_{cb}}] / \frac{D_{cb}}{2} = \frac{F_y R_{cby}}{k_{cb} D_{cb}^{\,2}}\ \vec{\imath} \quad (29)$$

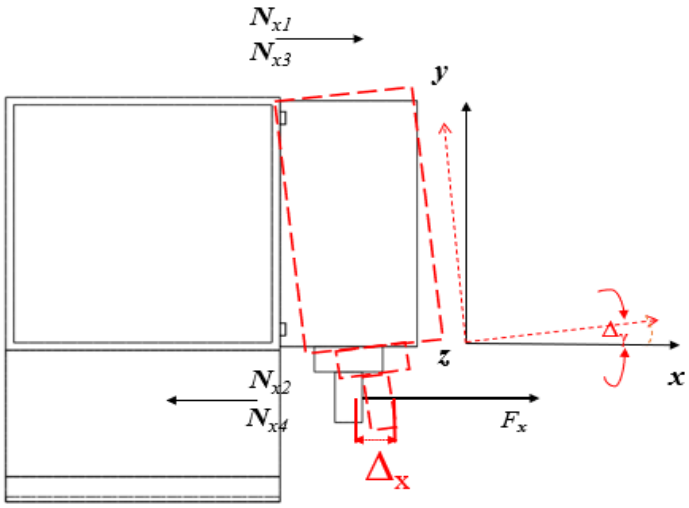

Figure 23 Side view of machine head deformation due to +X directional machining force.

After having both positional error and beam rotation under +Y directional force load (Fig.23), it is simple to follow the same logic to define the error under +X direction force load.

Given $Q_{x1}\vec{j} = Q_{x2}\vec{j} = Q_{x3}\vec{j} = Q_{x4}\vec{j} = + (\frac{F_x}{4})\vec{j}$, the positional error under +X directional force load will be:

$$\Delta x_{cbx} = \frac{F_x}{4k_{cbx}}\vec{\imath} \quad (30)$$

Given $N_{x1}\vec{\imath} = N_{x3}\vec{\imath} = [+ (\frac{F_x R_{cbx}}{2D_{cb}})\vec{\imath}]$, the beam rotation caused by +X directional force will be:

$$\Delta\gamma_{cbx} = [(\frac{F_x R_{cbx}}{2D_{cb}}) \times \frac{1}{k_{cb}}] / \frac{D_{cb}}{2} = \frac{F_x R_{cbx}}{k_{cbx} D_{cb}^{\,2}}\ \vec{\imath} \quad (31)$$

For cross beam deformation when +Z direction applied, they will be slightly complicated because the beam will experience two moments in different direction.

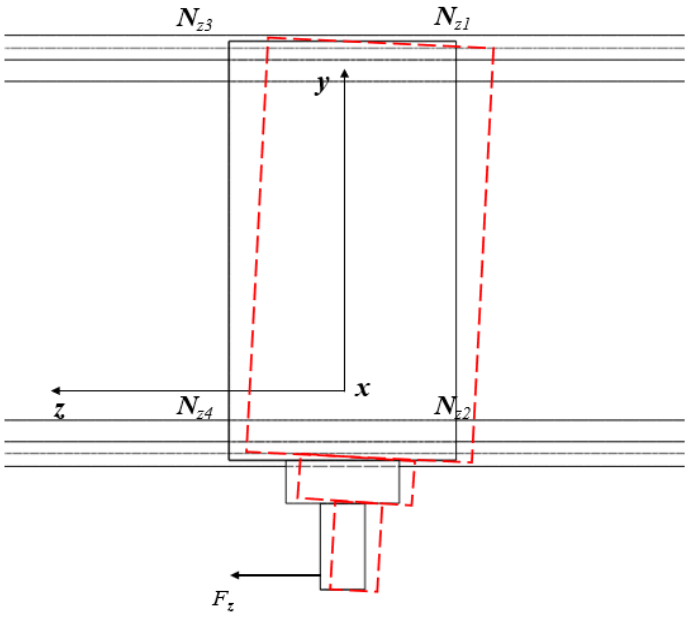

Figure 24 Front view of crossbeam deformation due to torque around X axis.

Moment of force on X axis (Fig.24):

$$N_{z1}\vec{j} = N_{z2}\vec{j} = [\ (\frac{F_z R_{cbz2}}{2L_{cb}})\ \vec{j}] \quad (32)$$

$$\Delta\alpha_{cbz} = [\ (\frac{F_x R_{cbz2}}{2L_{cb}}) \times \frac{1}{k_{cbz}}]/\ \frac{L_{cb}}{2} = \frac{F_z R_{cbz2}}{k_{cbz} {L_{cb}}^2}\ \vec{k} \quad (33)$$

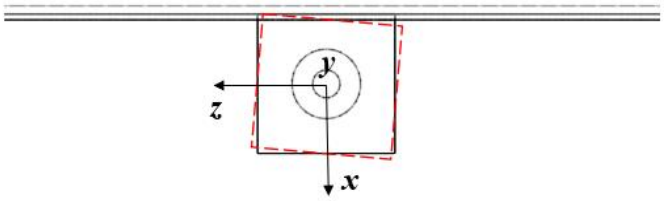

Figure 25 Top view of crossbeam deformation due to torque around Y axis.

Moment of force on Y axis (Fig.25):

$$N_{z1}\vec{i} = N_{z2}\vec{i} = [-\ (\frac{F_z R_{cbz1}}{2L_{cb}})\ \vec{i}] \quad (34)$$

$$\Delta\beta_{cbz} = [\ -\ (\frac{F_x R_{cbz1}}{2L_{cb}}) \times \frac{1}{k_{cbz}}]/\ \frac{L_{cb}}{2} = -\ \frac{F_z R_{cbz1}}{k_{cbz} {L_{cb}}^2}\ \vec{j} \quad (35)$$

3.4.3 Statics analysis for machine bed

After constructing the machining error model for cross beam based on stiffness. The crossbeam is attached on the machine bed, moves in X direction. Machining force will be transferred to machine beam through deformation of the crossbeam (Fig.26); therefore, it is

necessary to perform the study on machine bed deformation under machining force. The error model for machine bed will be identical to the cross beam, after re-define some quantities related to the displacement. The analysis of machine bed will be given as followed:

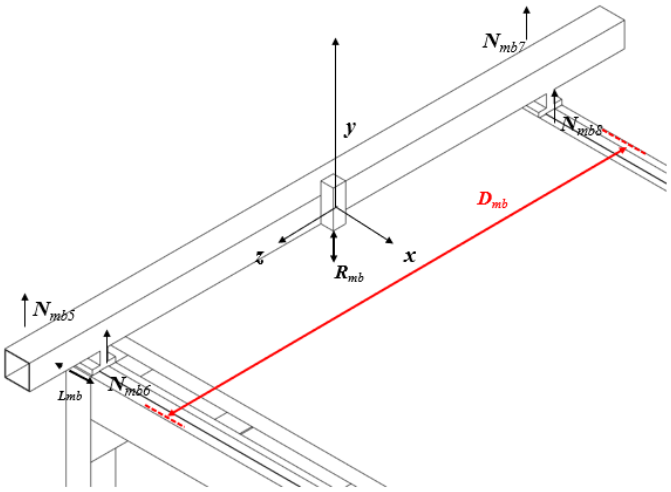

Figure 26 Side view of machine bed with crossbeam.

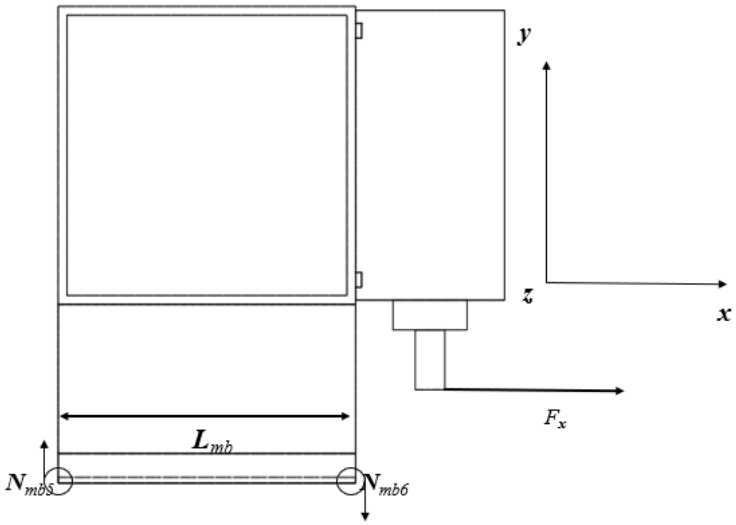

Figure 27 Side view of machine bed when +X directional machining force applied to tool.

For the machine bed, when a unit force at +X direction is applied (Fig.27), it can be treated as a force $+F_x \vec{\imath}$ and a moment of force $+M_{mby} \vec{\jmath}$, defining the displacement between the force and machine bed R_{mb}, the moment is the cross product of the displacement and force:

$$M_{mbx} \vec{k} = - R_{mb} \vec{\jmath} \times F_x \vec{\imath} \quad (36)$$

The moment of force can be treated as a force pair defined as:

$$\pm\left(\frac{M_{mbx}}{L_{mb}}\right) \vec{\jmath} \quad (37)$$

Rearranging the terms base on the definition of moment:

$$M_{mbx}\,\vec{k} = L_{mb}\,\vec{\imath}\,[-(\frac{M_{mbx}}{L_{mb}})\vec{J}] = L_{mb}\,\vec{\imath} \times 2[-(\frac{F_x R_{mb}}{2L_{mb}})\vec{J}] \quad (38)$$

L_{mb} is the spacing between two linkage point attached to the rail in Y direction, distance between point 5 and 6.

$$N_{x5}\vec{J} = N_{x7}\vec{J} = [-(\frac{F_x R_{mbx}}{2L_{mb}})\,\vec{J}] \quad (39)$$

$$N_{x6}\vec{J} = N_{x8}\vec{J} = [+(\frac{F_x R_{mbx}}{2L_{mb}})\,\vec{J}] \quad (40)$$

The shear force will be acting on guide screws on the machine bed when the direction of machining force is same as the crossbeam's movement, so when study on machine bed deformation the shear will not be included, same has been done when analyzing cross beam deformation.

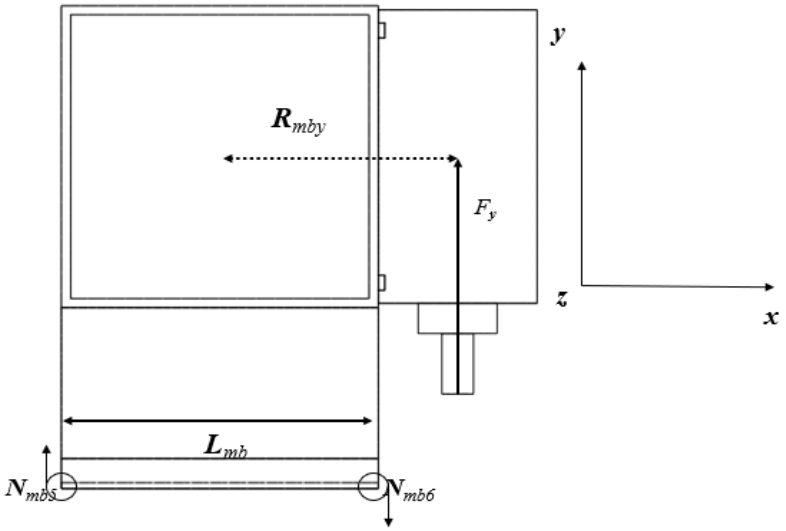

Figure 28 Side view of machine bed when +Y directional machining force applied to tool.

When a unit force at +Y direction (Fig.28) been applied to the machine bed, it can be seen as a force $+F_y\,\vec{J}$ and moment $M_{mby}\,\vec{k}$. Normal force will be demonstrated only considering the moment causing rotation on Z-axis.

$$N_{y5}\vec{J} = N_{y7}\vec{J} = [-(\frac{F_y R_{mby}}{2L_{mb}})\,\vec{J}] \quad (41)$$

$$N_{y6}\vec{J} = N_{y8}\vec{J} = [+(\frac{F_y R_{mby}}{2L_{mb}})\,\vec{J}] \quad (42)$$

$$Q_{y1}\,\vec{k} = Q_{y2}\,\vec{k} = Q_{y3}\,\vec{k} = Q_{y4}\,\vec{k} = (\frac{F_y}{4})\vec{J} \quad (43)$$

When a unit force at +Z direction been applied to the machine bed:

Moment around X axis:

$$N_{z5}\vec{J} = N_{z6}\vec{J} = [-(\frac{F_z R_{mb}}{2D_{mb}})\,\vec{J}] \quad (44)$$

$$Nz7\vec{j} = Nz8\vec{j} = [+ (\frac{F_z R_{mb}}{2D_{mb}})\ \vec{j}] \quad (45)$$

Moment around Y axis:

$$Nz5\vec{j} = Nz6\vec{j} = [+ (\frac{F_z R_{mby}}{2D_{mb}})\ \vec{i}] \quad (46)$$

$$Nz7\vec{j} = Nz8\vec{j} = [- (\frac{F_z R_{mby}}{2D_{mb}})\ \vec{i}] \quad (47)$$

$$Qz1\ \vec{k} = Qz2\ \vec{k} = Qz3\ \vec{k} = Qz4\ \vec{k} = (\frac{F_z}{4})\vec{k} \quad (48)$$

3.4.4 Correlation between deformation and machining force for machine bed

By applying the Hooke's Law to the machine bed and follow the same procedures as did for the cross beam, since the cross beam moves on the machine bed in X direction, so there will not be deformation in X direction for the machine bed when it experiences +X direction machining force. But +X directional force will cause the machine bend tends to rotate around the Z-axis, applying angle approximation, the rotation can be given:

$$\Delta\gamma mbx = [\ (\frac{F_x R_{mbx}}{2L_{mb}}) \times \frac{1}{k_{mbx}}]/\ \frac{L_{mb}}{2} = \frac{F_x R_{mb}}{k_{mbx} {L_{mb}}^2}\ (-\vec{i}) \quad (49)$$

When +Y direction machining force been applied, the machine bed will have following deformation:

$$\Delta ymby = \frac{F_y}{4k_{mby}}\vec{J} \quad (50)$$

$$\Delta\gamma mby = [\ (\frac{F_y R_{mby}}{2L_{mb}}) \times \frac{1}{k_{mby}}]/\ \frac{L_{mb}}{2} = \frac{F_y R_{mby}}{k_{mby} {L_{mb}}^2}\ (-\vec{i}) \quad (51)$$

When +Z direction machining force been applied, the machine bed will have following deformation:

$$\Delta zmbz = \frac{F_z}{4k_{mbz}}\vec{k} \quad (52)$$

$$\Delta\alpha mbz = [\ (\frac{F_z R_{mb}}{2D_{mb}}) \times \frac{1}{k_{mbz}}]/\ \frac{D_{mb}}{2} = \frac{F_y R_{mb}}{k_{mbz} {D_{mb}}^2}\ (\vec{k}) \quad (53)$$

$$\Delta\beta mbz = [\ (\frac{F_z R_{mby}}{2D_{mb}}) \times \frac{1}{k_{cbz}}]/\ \frac{D_{mb}}{2} = \frac{F_y R_{mby}}{k_{mbz} {D_{mb}}^2}\ (\vec{J}) \quad (54)$$

This study is only confused on parts deformation of crossbeam and machine bed since both have the highest priority when studying machining error deformation. The structure of machine head makes its deformation can be temporarily neglected.

Based on the correlation between parts deformation and machining force, aggregate equations for different parts that analyzed, one can get following equations to represent the machine tool deformation and parts rotation in different direction:

$$\Delta x = \frac{F_x}{4k_{cbx}}\vec{\imath} \qquad (55)$$

$$\Delta y = \frac{F_y}{4k_{cby}}\vec{J} + \frac{F_y}{4k_{mby}}\vec{J} \qquad (56)$$

$$\Delta z = \left(\frac{F_z}{4k_{mb}}\right)\vec{k} \qquad (57)$$

$$\Delta\alpha = \frac{F_x R_{cbz2}}{k_{cbz} D_{cb} L_{cb}}(\vec{k}) + \frac{F_y R_{mby}}{k_{mbz} {D_{mb}}^2}(\vec{k}) \qquad (58)$$

$$\Delta\beta = \frac{F_x R_{cbz1}}{k_{cbz} D_{cb} L_{cb}}(\vec{J}) + \frac{F_y R_{mby}}{k_{mbz} {D_{mb}}^2}(\vec{J}) \qquad (59)$$

$$\Delta\gamma = \frac{F_y R_{cby}}{k_{cb} {D_{cb}}^2}\vec{\imath} + \frac{F_x R_{cbx}}{k_{cbx} {D_{cb}}^2}\vec{\imath} + \frac{F_x R_{mb}}{k_{mbx} {L_{mb}}^2}(-\vec{\imath}) + \frac{F_y R_{mby}}{k_{mby} {L_{mb}}^2}(-\vec{\imath}) \qquad (60)$$

Chapter 4 Model Validation based on Numerical Simulation

4.1 Simulation setup and model simplification

This study will be conducted by using Fusion 360 from Autodesk to make comparison between physical (analytical) model and numerical simulation. From the error matrix, the crucial parameter will be focused on is tool-workpiece relative displacement. In physical machining error model, matrix [E_v] will represent this relative displacement, which is known as machining force induced error. In simulation software, a point will be selected based on the projection of the machine tool on the workpiece, the vector difference will be calculated by simulation software. In theory, after applying the machining force on the machine head in simulation software, the spacial coordinate of cutting tool will be different from its projection on workpiece due to the machining error. This comparison of the spacial coordinates of two points can be used to validate the physical model.

The simulation model is on a 3-axis high-speed milling machine given by the manufacturer and identical with the actual machine tool. The machine tool can be divided into the following main parts: machine bed, worktable, horizontal beam, machine head, spindle. The machine head moves in Z direction and crossbeam moves in X direction, all movement are being done by motors and guide screws. Spindle moves in Y direction completed by independent motor in machine head. Specific dimensional information and material selection are given in the table1 and 2 below.

Machine tool parts	**Dimension (L x W x H) (mm)**
Crossbeam	50 x 50 x 2620
Working Platform	2500 x 1600 x 60
Machine Head	50 x 50 x 75
Machine Bed Main Frame	2240 x 1245 x 605

Table 1 Dimensional specifications of 3-axis high-speed milling machine

Machine Parts	**Material**	**Hardness(B)**	**Density**	**Yield Stress**	**Elasticity**
Body Frame	ASTM A36	159	7.8g/cc	250Mpa	200Gpa
Crossbeam	ASM 6061	95	2.70g/cc	276Mpa	68.9Gpa
Slideway	ASTM 387	160	7.80g/cc	275Mpa	190Gpa
Platform	ASM 6061	95	2.70g/cc	276Mpa	68.9Gpa

Table 2 Material specification of 3-axis high-speed milling machine

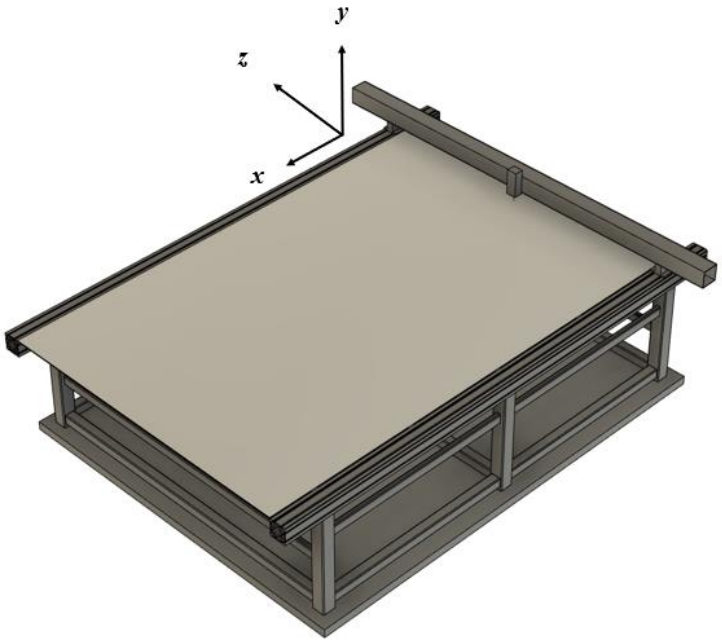

Figure 29 Simulation model for 3-axis high-speed milling machine.

After importing the model into simulation software, the first step will be model simplification. Eliminating bolt-nuts connection for the machine bed, remove the connection between guide screws and cross beam; smaller sized strengthening ribs are removed from the model. Then treating the machine head and spindle as a block by modifying the density of such block to match the actual weight of the head. Due to the working scenario of the milling machine which doesn't require Z-axis moving during the machining process because the thickness of the workpiece can be neglected. While model simplification can help to reduce computational cost and time, it can also lead to reduced accuracy in the simulation results. This is because simplifications may not capture all the details of the physical system being modeled and can introduce errors and uncertainties into the simulation [37,38]. In this case, removing the connection will ignore the material nonlinearity and assume force will be uniformly distributed on the machine tool. Since this study is focused on machining force induced error but not heavy-duty material removal process, so simplification will not affect the machine tool's structure integrity.

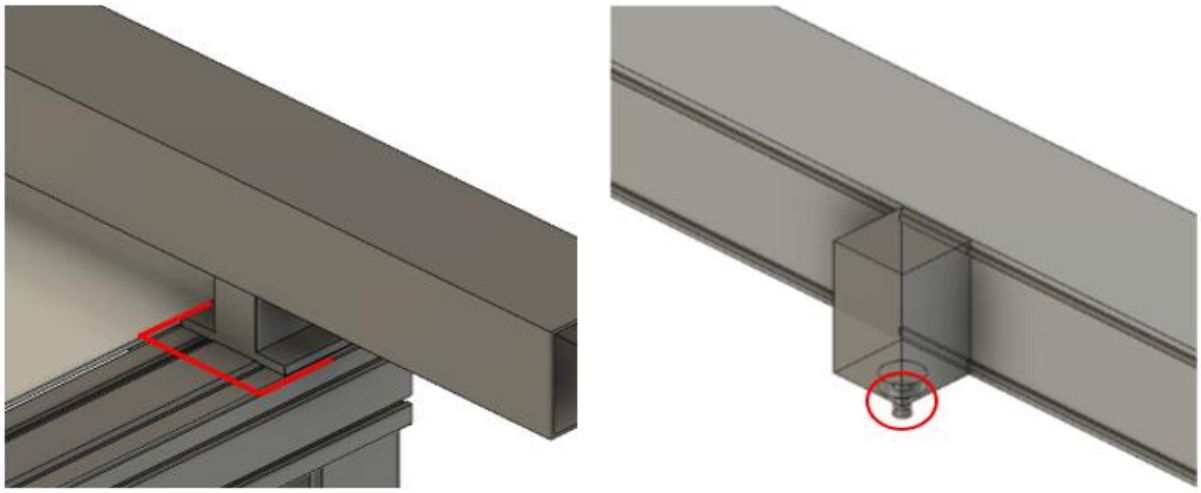

Figure 30 Model simplification on machine bed and machine head.

4.2 Loading

For every simulation in this study, gravitational force will be added to each model with value of 9.8m/s^2. Cross beam weighted 44kg, machine head including spindle and motor weighted 18kg, and working platform weighted 73.2kg. Machining force is a join force set to be -100N for X direction, 100N for Y direction and 100N for Z direction. The machining force is chosen to be 100N is due to the maximum loading acceptance for this specific model designing under its working condition. The direction of the joint XY directional force pointing at the center of upper quadrant area of the working platform. A repulsion force which is the same magnitude as machining force but opposite direction must be added on the worktable at position right beneath the spindle. The direction chosen is also because of matching the real-left working scenario.

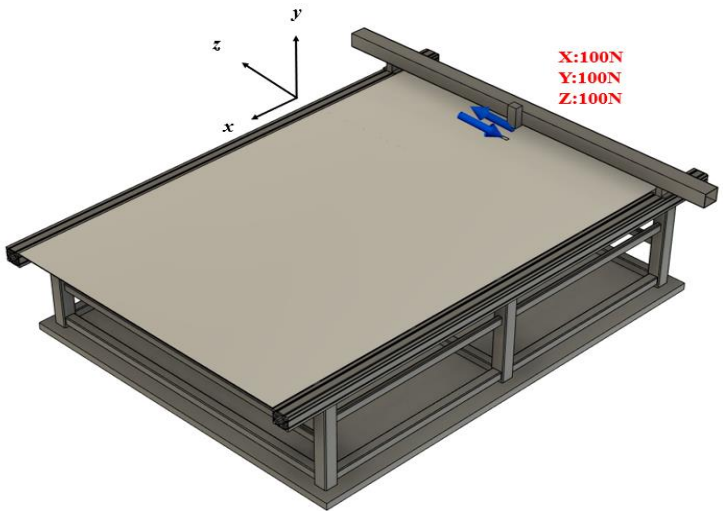

Figure 31 Loading condition for 3-axis high-speed milling machine.

4.3 Meshing and constrains

Set meshing type in fusion 360 as Tetrahedra, total 1,548,107 tetrahedra covers 100% of the volume, with face angle min: 1.57 max: 172. Worst shape ratio 95.6, worse aspect ratio 12.2, lowest collapse ratio 0.0151, worst Jacobian ratio 3.41, solver mesh has 2,854,201 nodes. In Fusion 360 simulation, the meshing density ratio refers to the control of the mesh size or element size in the simulation model. It allows one to adjust the density of the mesh to balance between computational efficiency and accuracy. The meshing density ratio determines the ratio of the element size to the maximum edge length in the geometry, provided number of tetrahedra corresponds to 8% meshing density which is also the most efficient for this machine tool model. Cross beam will move horizontally on the machine beam, this provides the transverse (X-axis) movement for the spindle over the workpiece. And machine head can move horizontally along the cross beam, which gives the spindle Y-axis movement. Machine head also has a motor mounted on the top, to allow the spindle moving along Y axis, but during the machining process, the Y direction movement is not required. Machine bed is fixed to the ground from X Y Z direction, and the cross beam is fixed at Y Z direction, allow it to move at X direction only during the machining process. The machine head is fixed at X Z direction, only allow to move at Y direction during the machining. The spindle will not move at any direction during the process.

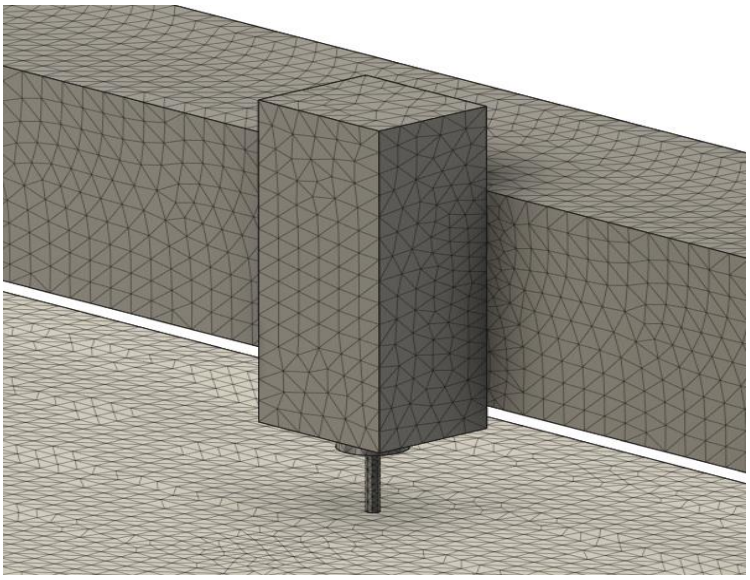

Figure 32 Generated Meshing with Tetrahedra type.

4.4 Type of contact

In the simulation software, there are three types of contact which are commonly used: sliding, rough, and bounded. Bounded are used between the parts connection using bolt-nuts, rough are used when frictional force is considered, sliding is the contact relation which don’t consider frictional force and used between the slider and rail. In this study, the contact relation between rail and cross beam is sliding, the rails are fixed on the machine bed using

bounded relation. The working platform which is used to hold the workpiece is also bounded with the machine's main frame. The machine tool is fixed on the ground using rough contact relation to mimic during the operation with the fractional force between bed and floor no matter how far the machine tool move will, since in this design there will not be bolts-nuts holding the machine bed with concrete floor. The machine head is also bounded with the beam because analyzing machining force will take place when the machine head and cross beam stop at pointed position.

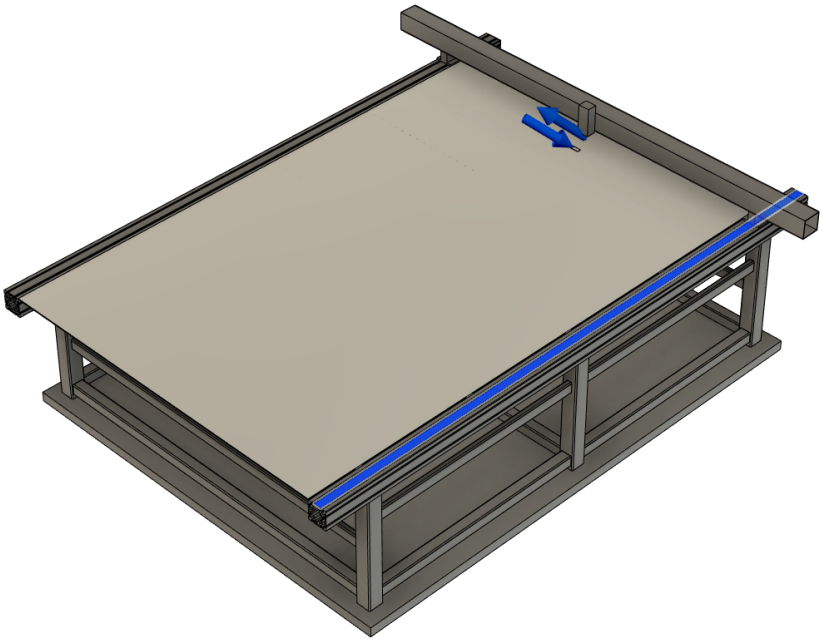

Figure 33 Contact condition between crossbeam and machine bed.

Bodies	Contact Set	Contact Type	Presentation Type
Left Rail	Sliding62	Sliding	Symmetric
Left Rail	Sliding63	Sliding	Symmetric
Left Rail	Sliding64	Sliding	Symmetric
Left Rail	Bonded80	Bonded	Symmetric
Left Rail	Bonded83	Bonded	Symmetric
Left Rail	Bonded99	Bonded	Symmetric

Table 3 Table for contact relation between machine bed and crossbeam.

4.5 Material

The main frame of the machine bed is manufactured with Q235 steel, which is equivalent to US standard ASTM A36 steel. Q235 steel has its minimum yield strength 250 MPa tested with steel diameter ≤ 16mm. Q235 steel has good plasticity, toughness, and weldability, as well as a certain strength, good cold bending performance. Crossbeam, machine head and working platform is made from 6061 aluminum alloy, it is one of the most widely used alloys. The main alloying elements are magnesium and silicon. It is a heat-treated wrought alloy, the temper designations mainly have 6061-T4, 6061-T6, etc. Aluminum 6061-T6 has a minimum yield strength of 276MPa, which is almost equal to that of A36 steel used in machine main frame, the strength combining with light weight, makes it perfectly suitable for applications where static loads are considered. The slideway is manufactured out of ASTM 387 steel, which has very similar mechanical properties as A36 steel used in the machine tool frame. It has Yield tensile stress of 275Mpa.

Chapter 5 Results & Discussion

5.1 Stiffness coefficients of each functional units

Stiffness coefficients of each component will be calculated deploying length-deformation method through simulation software in this study. Each component will be separated from the machine tool, in analysis of cross beam's stiffness coefficient, the machine head will be bounded on the cross beam, this is because the machine head (spindle motor) is mounted on bearings that are separate from the machine structure and is designed to generate rotational motion with minimal vibration and deflection. Furthermore, the machine head is equipped with a tool holder and cutting tool which are both relatively small in comparison to the machine structure.

Using cross beam as an example to find the parts stiffness coefficients, then other functional units such as machine bed can apply the same logic. Separate the cross beam from the whole machine tool and import it into a new statics analysis simulation task, constrains will be applied and contact method will all be bounded relation to mimic the structural integrity. After model simplification, by bounding the machine head with cross beam at beam's geometrical center position, then constrains will be added, the linking plates between beam and rails will be fixed in all X Y Z direction to simulate the condition which cross beam moves to a certain machining location and statics analysis can be conducted at this instantaneous time. Appling a machining force on the surface of the machine head, in this study the machining force starts at 100N since it is suggest by the machine tool manufacturer base on the working condition of this product, deformation of the beam will happen after the machining force has been applied, choose the geometrical center point on the surface which the force has been applied on, software will calculate the displacement of that point moves before and after applying machining force. When having the displacement, and knowing the machining force, stiffness coefficient can be calculated by using Hooke's Law. Repeat the same procedures for Y and Z directional machining force to get stiffness coefficients for cross beam in each direction.

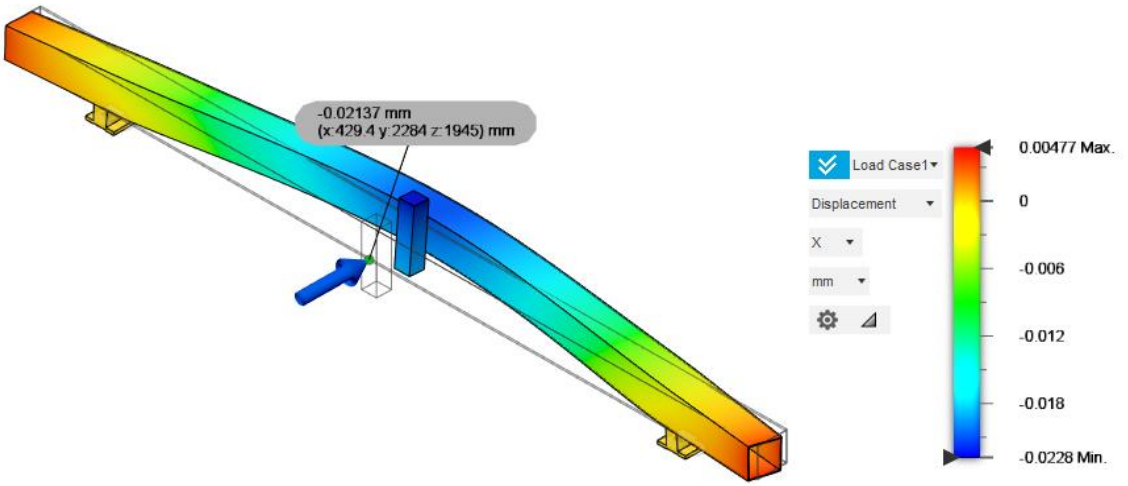

a)

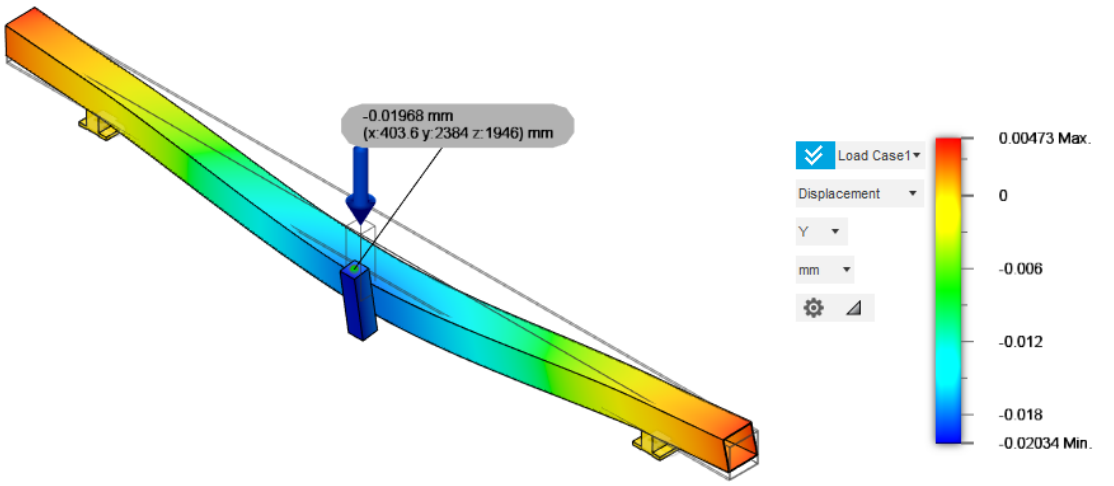

b)

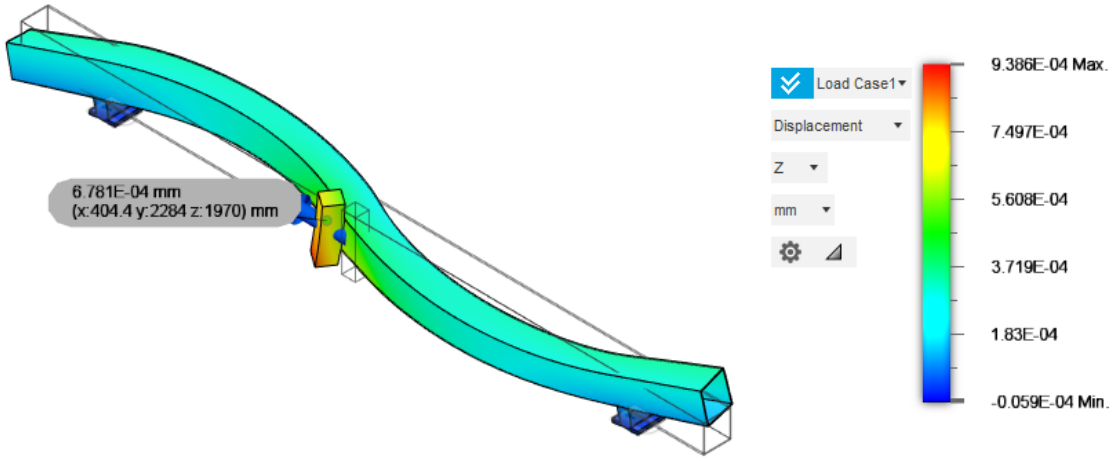

c)

Figure 34 a) Crossbeam deformation with +X direction force applied to machine head.

b) Crossbeam deformation with +Y direction force applied to machine head.

c) Crossbeam deformation with +Z direction force applied to machine head.

Above figures show the way of retrieving different directional stiffness coefficient for cross beam. By separating this functional unit, and apply the same constrains for different loading condition, the deformation in each direction is shown on the pictures, utilizing Hooke's Law to get the stiffness coefficient k_{cb} for each direction.

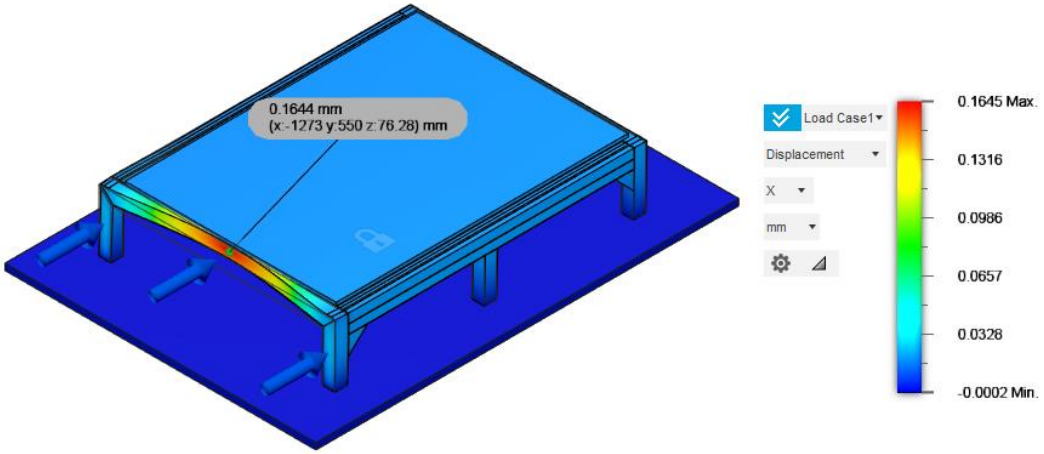

a)

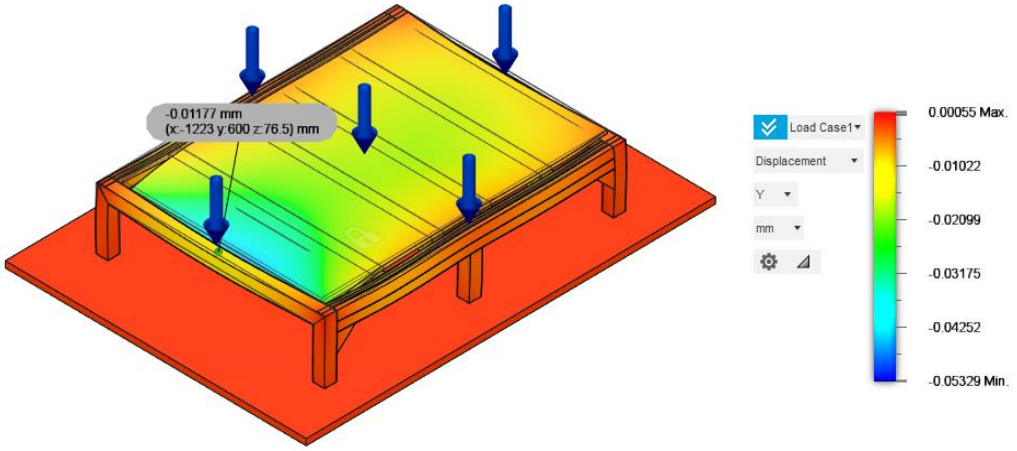

b)

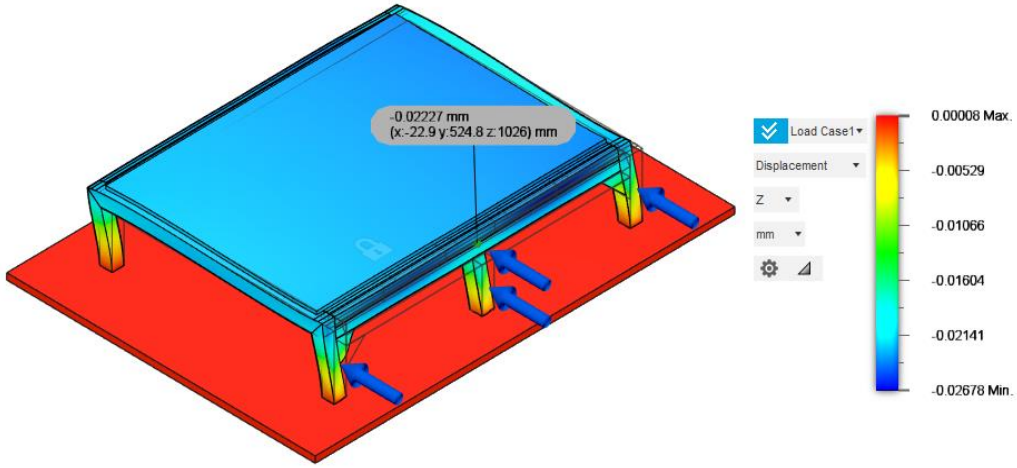

c)

Figure 35 a) Machine bed deformation with +X direction force applied to machine head.

b) Machine bed deformation with +Y direction force applied to machine head.

c) Machine bed deformation with +Z direction force applied to machine head.

The stiffness coefficient for machine bed is calculated in same manner, for all three directions. With the stiffness coefficient, K value, through statics analysis one can easily know the parts deformation based on Hooke's Law when given machining force, and by putting the positional and angular error generated under the machining force into the error matrix, the force induced machining error can be found through matrix [E_v].

K for crossbeam	Value (N/mm)	K for Machine bed	Value (N/mm)
k_{cbx}	4679	k_{mbx}	6079
k_{cby}	4926	k_{mby}	84962
k_{cbz}	142857	k_{mbz}	37341

Table 4 Static Stiffness for crossbeam and machine bed.

5.2 Machine tool parts deformation based on stiffness value

The way of retrieving stiffness coefficient for functional parts or assembly is done thorough simulation software, but stiffness for other standard units like guide screws can be obtained from manufacture's manuals. When having above coefficient, K values, one can follow the formulations from chapter 3 to calculate both rotational errors and positional errors.

For cross beam, under +Y directional force, the positional error caused by shear force can be defined as:

$$\Delta y_{cby} = \frac{F_y}{4k_{cby}}\vec{J} = 0.005075 \text{ mm} \quad (61)$$

Which is the same representation $\delta_{y2}(z)$, horizontal straightness error for assembly in coordinate system 1, as indicated in the deformation matrix in chapter 3. Subscript "2" stands for the correlation between coordinate system transforming is from O_2 to O_1, known as machine head to crossbeam. The "z" in the parenthesis means the motion is happening in Z direction when machine head moves along cross beam.

When +Y directional force applied, the torque will create beam rotation with angle $\Delta\gamma_{cby}$, which will further create positional errors in both X and Y direction, represented by $\varepsilon_{z2}(z)$ in error matrix. The way to calculate positional change due to the beam rotation is using small angle approximation, multiply the angle by respective distance from the force to each axis.

$$\Delta\gamma_{cby} = [\ (\frac{F_y R_{cby}}{2D_{cb}}) \times \frac{1}{k_{cby}}]/\ \frac{D_{cb}}{2} = \frac{F_y R_{cby}}{k_{cb} y D_{cb}{}^2}\ \vec{\imath} = \frac{100*75}{4926*100^2} = 0.000152 \quad (62)$$

$$Y: \Delta\gamma_{cby} \times 75\text{mm} = 0.0108 \text{ mm} \quad (63)$$

$$X: \Delta\gamma_{cby} \times 40\text{mm} = 0.00608 \text{ mm} \quad (64)$$

When +X directional force has been applied, there is also one positional error and one rotational error been created, the positional error is represented by $\delta_{x2}(z)$ in transformation matrix, and rotational error can be represented by $\varepsilon_{z2}(z)$.

$$\Delta x_{cbx} = \frac{F_x}{4k_{cbx}}\vec{\imath} = 0.005343 \text{ mm} \quad (65)$$

$$\Delta\gamma_{cbx} = \left[\left(\frac{F_x R_{cbx}}{2D_{cb}}\right) \times \frac{1}{k_{cb}} \right] / \frac{D_{cb}}{2} = \frac{F_x R_{cbx}}{k_{cbx} {D_{cb}}^2}\vec{\imath} = \frac{100*40}{4679*100^2} = 0.000085 \quad (66)$$

$$Y: \Delta\gamma_{cby} \times 75\text{mm} = 0.006375 \text{ mm} \quad (67)$$

$$X: \Delta\gamma_{cby} \times 40\text{mm} = 0.0034 \text{ mm} \quad (68)$$

When +Z directional force has been applied, there is also no positional error, but two rotational error been created, rotational error can be represented by $\varepsilon_{x2}(z)$ and $\varepsilon_{y2}(z)$.

$$\Delta\alpha_{cbz} = \left[\left(\frac{F_x R_{cbz2}}{2L_{cb}}\right) \times \frac{1}{k_{cbz}} \right] / \frac{L_{cb}}{2} = \frac{F_x R_{cbz2}}{k_{cbz} {L_{cb}}^2}\vec{k} = 0.000011 \quad (69)$$

$$Z: \Delta\alpha_{cbz} \times 75\text{mm} = 0.000825 \text{ mm} \quad (70)$$

$$Y: \Delta\alpha_{cbz} \times 40\text{mm} = 0.00044 \text{ mm} \quad (71)$$

$$\Delta\beta_{cbz} = -\left[\left(\frac{F_x R_{cbz1}}{2L_{cb}}\right) \times \frac{1}{k_{cbz}} \right] / \frac{L_{cb}}{2} = -\frac{F_x R_{cbz1}}{k_{cbz} {L_{cb}}^2}\vec{\jmath} = -0.000021 \quad (72)$$

(In case which spindle rotates around Y axis, will cause no change of tool's coordinate.)

For machine bed, the coordinate system will transfer from O_1 to O_0, first calculating the rotation of the machine bed when +X directional force has been applied on the machine head, which is equivalent to $\varepsilon_{z1}(x)$.

$$\Delta\gamma_{mbx} = \left[\left(\frac{F_x R_{mbx}}{2L_{mb}}\right) \times \frac{1}{k_{mbx}} \right] / \frac{L_{mb}}{2} = \frac{F_x R_{mb}}{k_{mbx} {L_{mb}}^2}(-\vec{\imath}) = \frac{100*10}{6079*100^2} = -0.000016 \quad (73)$$

$$Y: \Delta\gamma_{mbx} \times 75\text{mm} = 0.006375 \text{ mm} \quad (74)$$

$$X: \Delta\gamma_{mbx} \times 20 \text{ mm} = 0.00032 \text{ mm} \quad (75)$$

When +Y directional force has been applied on the machine head, machine bed will experience a positional error created by shear force and a rotation, which can be represented by $\delta_{x1}(x)$ and $\varepsilon_{z1}(x)$ in transformation matrix:

$$\Delta y_{mby} = \frac{F_y}{4k_{mby}}\vec{\jmath} = 0.000294 \text{ mm} \quad (76)$$

$$\Delta\gamma_{mby} = \left[\left(\frac{F_y R_{mby}}{2L_{mb}}\right) \times \frac{1}{k_{mby}} \right] / \frac{L_{mb}}{2} = \frac{F_y R_{mby}}{k_{mby} {L_{mb}}^2}(-\vec{\imath}) = -\frac{100*75}{84962*100^2} = -0.000009 \quad (77)$$

For machine bed, the deformation caused by rotation can be neglected from now on. Because of the magnitude of angle which rotates is extremely small, the positional change caused by such rotation will not affect the result significantly.

When +Z directional force has been applied on the machine head, machine bed will experience a positional error and two rotational errors, which can be represented by $\varepsilon_{z1}(x)$ and $\varepsilon_{x1}(x)$, $\varepsilon_{y1}(x)$ in transformation matrix:

$$\Delta z_{mbz} = \frac{F_z}{4k_{mbz}}\vec{k} = 0.00067 \text{ mm} \quad (78)$$

$$\Delta\alpha_{mbz} = \left[\left(\frac{F_z R_{mb}}{2D_{mb}}\right) \times \frac{1}{k_{mbz}} \right] / \frac{D_{mb}}{2} = \frac{F_y R_{mb}}{k_{mbz} {D_{mb}}^2}(\vec{k}) = \frac{100*20}{37341*1800^2} = 1.65\text{e-}08 \quad (79)$$

$$\Delta\beta_{mbz} = \left[\left(\frac{F_z R_{mby}}{2D_{mb}}\right) \times \frac{1}{k_{cbz}} \right] / \frac{D_{mb}}{2} = \frac{F_y R_{mby}}{k_{mbz} {D_{mb}}^2}(\vec{j}) = \frac{100*75}{37341*1800^2} = 6.2\text{e-}08 \quad (80)$$

5.3 Comparison of theoretical machining error with simulation result (model validation)

With the calculated statics stiffness value from chapter 5.1, physical modeling can give the force-induced machining error of the 3-axis high-speed milling machine in each direction. Using direct measurement method to verify the physical (analytical) model is frequently used in model verification, but there are still references [39,40,41] which adopt numerical simulations to verify the analytical model. Since there is a lack of real machine tool and test equipment, numerical simulation of the studied machine tool will be used to calculate the machining error and compare with analytical model.

Statics analysis models are constructed when crossbeam is at starting position, left starting point of the machine tool. The machine head is at the center of the beam. Since the Y axis movement of spindle is not required during the machining process, the transformation matrix relating to the spindle will be identity matrix. For the workspace, neglecting the errors from machine bed to workpiece by using identity matrix for $[{}^0T'_w]$. The force induced error can be demonstrated by the formulation in chapter 3, $[E_v] = [{}^0T'_t]^{-1}\,[{}^0T'_w]$

Results for machining error in each direction are given:

X: 0.01516 mm

Y: 0.022 mm

Z: 0.0015 mm

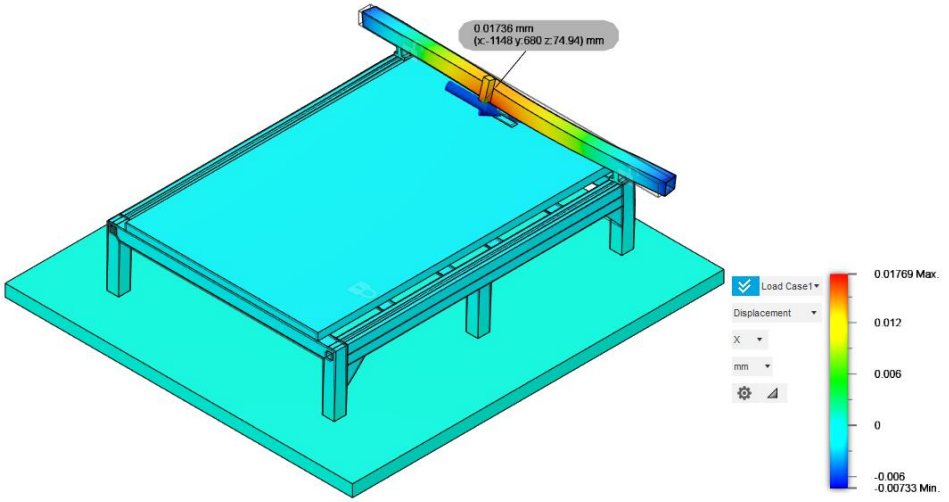

a)

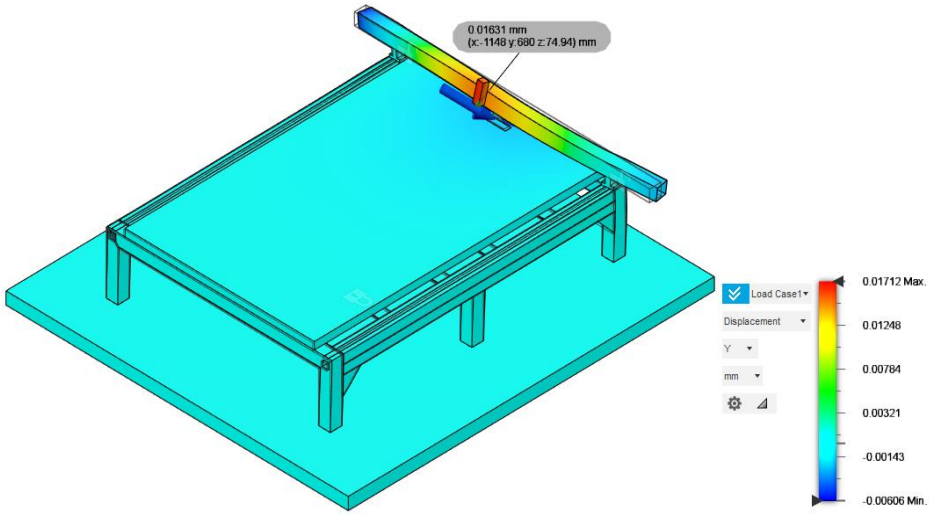

b)

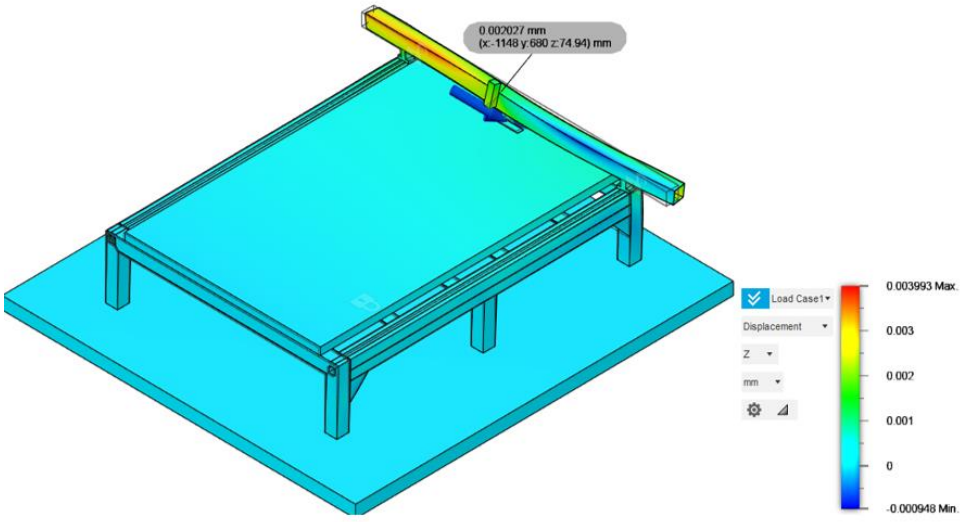

c)

Figure 36 a) machine tool deformation in X direction under machining force

b) machine tool deformation in Y direction under machining force

c) machine tool deformation in Z direction under machining force

The final step of error comparison is to get machine tool deformation result in simulation software. Importing the whole machine tool model, apply machining force to the tool tip with following parameters, 100N for Fx, 100N Fy, 100N Fz and add a repulsion force on the workspace which has -100N for all directions. Gravitational force is excluded to make the result consistent with physical model. Calculating the positional change at the cutting tool tip in X, Y, Z direction:

X: 0.01736 mm

Y: 0.01631 mm

Z: 0.002027 mm

Theoretical deformation (mm)	**Simulation deformation (mm)**	**error**
X: 0.01516	0.01736	14.5%
Y: 0.022	0.01631	25.86%
Z: 0.0015	0.00203	21.7%

Table 5 Comparison between theoretical result and simulated result

The result from physical modeling has been given in the first column from the table above, the model calculated the theoretical value of tool-workpiece deformation (force-induced machining error) in X, Y, Z direction. The model corelates the relationship between force-induced machining error and static stiffness of each machine tool part. With the static stiffness calculated using length-deformation method in simulation software, model can give theoretical force-induced machining error from each direction.

From the result in above table, the error between simulated deformation and theoretical deformation varies from 14.5% to 25.86%, the limit of acceptable error between numerical simulation and physical simulation depends on the specific application and the desired level of accuracy. In related studies on machine tool error modeling and prediction, the error between direct measurement and simulation model has 25% error [42]. The working condition for this 3-axis high-speed milling machine given by machine tool manufacturer, requires accuracy level within 0.1mm, this physical model is acceptable.

The error between analytical modeling calculations and numerical simulation can be believed to be the way of retrieving machine tool parts structural stiffness. The stiffness value of machine tool parts used in physical modeling calculation is by performing length-deformation method. But when using numerical simulation to calculate force-induced machining error, the software performs the calculation for stiffness and other factors based on material property in its database, which typically includes behavior of real material, such as nonlinearity and anisotropy.

In this study, when a positive 100N machining force is given in all three directions, the positive Y directional machining error contributes the most with its value 0.022mm. With only numerical simulation result, it is hard to explain which factor leads to this directional machining error, but now with the analytical modeling, it is obvious to tell from equation (63) the crossbeam rotation towards positive Y direction contributes the most towards machining error in Y direction. Furthermore, from equation (63), since the small angle approximation has been applied, one can quickly tell the most effective way to minimize this direction machining error is to reduce the height of the machine head. When designing or performing structural optimization, the suggestion from physical modeling will be adding the horizontal supporting structural inside the crossbeam to avoid its deformation in Y direction when machining force applied.

From this example it is evident that physical modeling provides a more accurate and precise understanding of the machine tool's behavior, as well as identify sources of error that may be difficult to simulate in a numerical model.

Chapter 6 Conclusion and future scope

In this thesis, a physical (analytical) error model has been established by utilizing traditional homogenous error transformation matrix. The machine tool deformation has been studied by applying classic statics analysis. With the combination of statics analysis and mathematical error transformation matrix, a new physical model representation of machining-force-induced error has been investigated. The machining (tool-workpiece displacement) error can be calculated by the proposed model with known machining forces.

One application of the proposed model can be the machining-force-induced error calculation for crossbeams in a 3-axis machine tool, where torque generated by machining force dominates the deformation of such setup compare with tangential force created by machining process. This gives an insight to improve the rotor resistance while conducting topological optimization of such machine tool crossbeam.

Another application of the proposed model can be the machining-force-induced error calculation for bed part. The torque created by machining force hardly caused any influence due to the size of this machine bed. Tangential force, or shear force in this case has greater contribution towards the deformation of machine bed. Increasing shear strength should be taken into consideration when optimizing such machine bed.

In future study, the model can be improved by considering the deformation of transmission devices such as guide screws so as to investigate the deformation of such parts resulting in the deformation of the whole machine tool, affects the machining error. Direct measurement method can be applied to further validate the physical model when the real machine and test equipment is reachable.

References

[1] “Machine Tools Market Size, Share & Growth Report, 2030.” Machine Tools Market Size, Share & Growth Report, 2030.

[2] “US Machine Tools Market Size, Share | 2022 - 27 | Industry Report, Growth.” Mordor intelligence, www.mordorintelligence.com/industry-reports/united-states-machine-tools-market. Accessed 26 Aug. 2022.

[3] Zhu, S., Ding, G., Qin, S., Lei, J., Zhuang, L., & Yan, K. (2012). Integrated geometric error modeling, identification and compensation of CNC Machine Tools. International Journal of Machine Tools and Manufacture, 52(1), 24–29.

[4] A.C. Okafor, Y.M. Ertekin, Derivation of machine tool error models and error compensation procedure for three axes vertical machining center using rigid body kinematics, Int. J. Mach. Tool Manuf. 40 (2000) 1199–1213.

[5] S.P. Su, S.Y. Li, G.L. Wang, Identification method for errors of machining center based on volumetric error model, Chin. J. Mech. Eng. 38 (2002) 121–125 in Chinese.

[6] Y.Y. Hsu, S.S. Wang, A new compensation method for geometry errors of five axis machine tools, Int. J. Mach. Tool Manuf. 47 (2007) 352–360

[7] W.T. Lei, Y.Y. Hsu, Error measurement of five-axis CNC machines with 3D probe-ball, J Mater. Process. Tech. 139 (2003) 127–133.

[8] S.H. Suh, E.S. Lee, J.W. Sohn, Enhancement of geometric accuracy via an intermediate geometrical feedback scheme, J. Manuf. Syst. 18 (1999) 12–21.

[9] M. Rahman, J. Heikkala, K. Lappalainen, Modeling, measurement and error compensation of multi-axis machine tools. Part I: theory, Int. J. Mach. Tool Manuf. 40 (2000) 1535–1546.

[10] W.T. Lei, Y.Y. Hsu, Accuracy enhancement of five-axis CNC machines through real-time error compensation, Int. J. Mach. Tool Manuf. 43 (2003) 871–877

[11] J.W. Fan, J.L. Guan, W.C. Wang, Q. Luo, X.L. Zhang, L.Y. Wang, A universal modeling method for enhancement the volumetric accuracy of CNC machine tools, J Mater. Process. Technol. 129 (2002) 624–628.

[12] S. Suh, E. Lee and S. Jung, “Error modelling and measurement for the rotary table of five-axis machine tools”, International Journal of Advanced Manufacturing Technology, 14, pp. 656– 663, 1998.

[13] J. A. Soons, F. C. Theuws and P. H. Schllekens, “Modeling the errors of multi-axis machines: a general methodology”, Precision Engineering, 14(1), pp. 5–19, 1992.

[14] P. D. Lin and K. F. Ehmann, “Direct volumetric error evaluation for multi-axis machines”, International Journal of Machine Tools and Manufacture, 33(5), pp. 175–693, 1993.

[15] Lin, Y. and Shen, Y., 2003. Modelling of Five-Axis Machine Tool Metrology Models Using the Matrix Summation Approach. *The International Journal of Advanced Manufacturing Technology*, 21(4), pp.243-248.

[16] V. S. B. Kiridena and P. M. Ferreira, “Mapping of the effects of positioning errors on the volumetric accuracy of five-axis CNC machine tools”, International Journal of Machine Tools and Manufacture, 33(3), pp. 417–437, 1993.

[17] Srivastava, A. K., Veldhuis, S. C., & Elbestawit, M. A. (1995). Modelling geometric and thermal errors in a five-axis CNC Machine Tool. International Journal of Machine Tools and Manufacture, 35(9), 1321–1337.

[18] Ferreira PM, Liu CR (2008) An analytical quadratic model for the geometric error of a machine tool. In: Journal of Manufacturing Systems.

[19] P. Dufour, R. Groppetti. "Computer Aided Accuracy Improvement in Large NC Machine Tools," Proceedings of the 22nd International MTDR Conference, 1981.

[20] T. Sata, Y. Takeuchi, N. Okubo. "Improvement of Working Accuracy of a Machining Center by Computer Control Compensation," Proceedings of the 18th International MTDR Conference, 1977.

[21] W.J. Love, A.J. Scarr, "The Determination of the Volumetric Accuracy of Multi-Axis Machines," Proceedings of the 14th International MTDR Conference, 1973.

[22] R. Hocken, et al. "Three-Dimensional Metrology," Annals of CIRP, Volume 26, 1977.

[23] V.T. Portman. "Error Summation in the Analytical Calculation of Lathe Accuracy," Stanki i Instrument, Volume 50, No. 1, 1980.

[24] A. Donmez. "'Total Software Error Compensation of a Turning Center," Progress Report #4 submitted to the National Bureau of Standards, School of Industrial Engineering, Purdue University, West Lafayette, Indiana, 1983.

[25] A. Donmez, D. Blomquist, C.R. Liu, R. Hocken, M.M. Barash."A General Mathematical Model for the Calculation of the Total Error Map of a Machine-Tool with Application to Turning Centers," (to be submitted for publication in Precision Engineering).

[26] Portman VT, Chapsky VS, Shneor Y, Ayalon E (2015) Machine stiffness rating: characterization and evaluation in design stage. Procedia CIRP 36:111–116

[27] Vrtiel Š, Hajdu Š, Behúlová M (2017) Analysis of the machine frame stiffness using numerical simulation. IOP Conf Ser Mater Sci Eng 266:012015.

[28] Suh JD, Lee DG, Kegg R (2002) Composite machine tool structures for high-speed milling machines. CIRP Ann Manuf Technol 51:285–288.

[29] Cui, Yi, et al. “An Accurate Thermal Performance Modeling and Simulation Method for Motorized Spindle of Machine Tool Based on Thermal Contact Resistance Analysis.” The International Journal of Advanced Manufacturing Technology, vol. 96, no. 5–8, 2018, pp. 2525–2537.

[30] Zhang, Fei, et al. “Structure Analysis and Optimization for High-Speed Vertical Machining Tool Table.” Applied Mechanics and Materials, vol. 120, 2011, pp. 197–202.

[31] Monkova, K., Monka, P., Tkac, J., Hricova, R., & Mandulak, D. (2019). Effect of the weight reduction of a gear wheel on modal characteristics. MATEC Web of Conferences, 299, 03002.

[32] ISO. Test Code for Machine Tools—Part 1: Geometric Accuracy of Machines Operating under No-Load or Quasi-Static Conditions; ISO 230-1; ISO: Geneva, Switzerland, 2012.

[33] ISO. Test Code for Machine Tools—Part 7: Geometric Accuracy of Axes of Rotation; ISO 230-7; ISO: Geneva, Switzerland, 2015.

[34] Li, Hui-qin, et al. “Research on Precision of Modular Machine Tool Based on Computer Aided Multi-Body System Method.” Cluster Computing, vol. 22, no. S4, Springer Science and Business Media LLC, Mar. 2018, pp. 9145–50.

[35] Cong, Dang Chi et al. "Volumetric Error Model for Multi-Axis Machine Tools". Procedia Manufacturing, vol 1, 2015, pp. 1-11. Elsevier BV.

[36] Team, Travers. “How to Reduce or Eliminate Chatter in Machining.” How to Reduce or Eliminate Chatter in Machining, https://solutions.travers.com/metalworking-machining/milling/how-to-reduce-or-elminate-chatter-in-machining.

[37] Huang, Tao, et al. “A Survey of Modeling and Control in Ball Screw Feed-Drive System.” The International Journal of Advanced Manufacturing Technology, vol. 121, no. 5–6, 2022, pp. 2923–2946, doi:10.1007/s00170-022-09506-4.

[38] Chen, J.-S., et al. “Mechanical Model and Contouring Analysis of High-Speed Ball-Screw Drive Systems with Compliance Effect.” The International Journal of Advanced Manufacturing Technology, vol. 24, no. 3–4, 2004, doi:10.1007/s00170-003-1777-9.

[39] Li, Yang, et al. “A Review on Spindle Thermal Error Compensation in Machine Tools.” International Journal of Machine Tools and Manufacture, vol. 95, 2015, pp. 20–38,

[40] Sanchez, J.A., et al. “Experimental and Numerical Study of Angular Error in Wire-EDM Taper-Cutting.” International Journal of Machine Tools and Manufacture, vol. 48, no. 12–13, 2008, pp. 1420–1428

[41] Haitao, Zhao, et al. “Simulation of Thermal Behavior of a CNC Machine Tool Spindle.” International Journal of Machine Tools and Manufacture, vol. 47, no. 6, 2007, pp. 1003–1010, doi:10.1016/j.ijmachtools.2006.06.018.

[42] Zhang, Yi, et al. “Machine Tool Thermal Error Modeling and Prediction by Grey Neural Network.” The International Journal of Advanced Manufacturing Technology, vol. 59, no. 9–12, 2011, pp. 1065–1072